FEEDSTOCK ADDITIVES IN GASIFICATION

Effect on Ash Sintering Behaviour
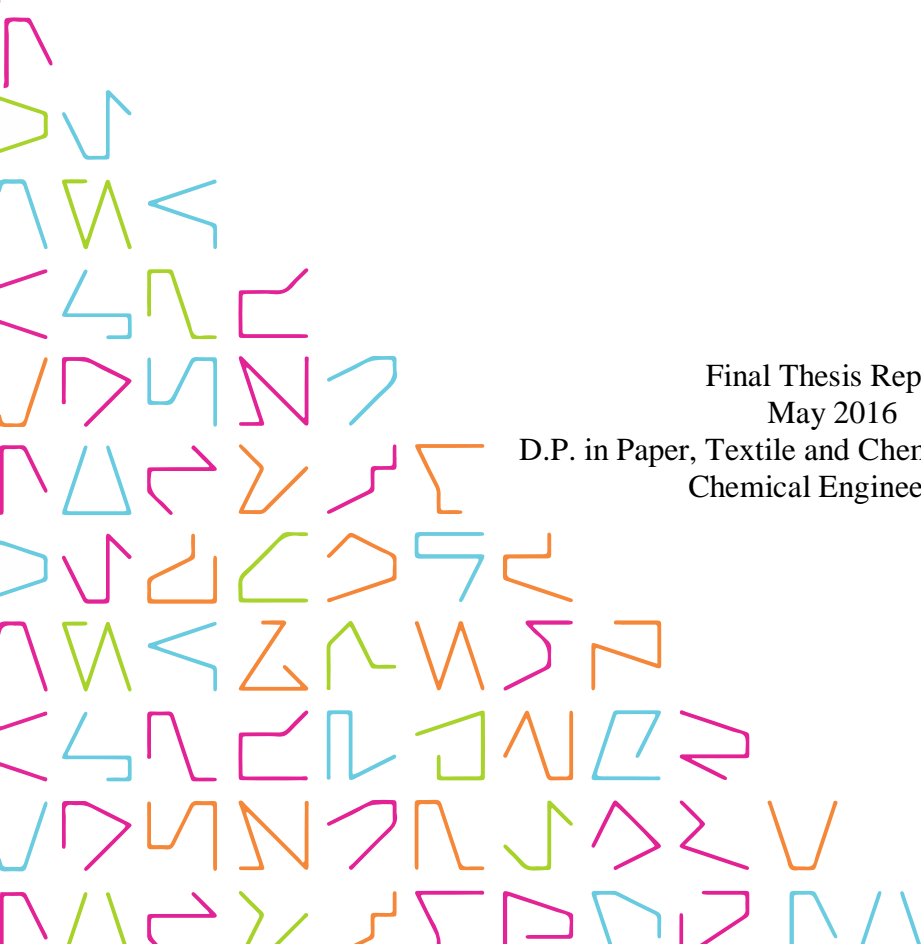## in Wheat Straw Gasification

Patrik Eskelinen

ABSTRACT

Tampereen ammattikorkeakoulu
Tampere University of Applied Sciences
Degree Programme in Paper, Textile and Chemical Engineering
Chemical Engineering

ESKELINEN PATRIK:
Feedstock Additives in Gasification
Effect on Ash Sintering Behaviour in Wheat Straw Gasification

Bachelor's thesis 37 pages, appendices 4 pages
May 2016

In this thesis work the effects of kaolin and magnesium oxide on the ash sintering behaviour of wheat straw in gasification was studied. Small scale gasification of agricultural biomass wastes, or crop residues such as wheat straw, presents a case of clear economic and environmental advantage possibly reducing by over 90 % greenhouse gas emissions if compared with the use of fossil fuels.

This work supported deployment of bench-scale tests for the development of fixed-bed gasification solutions by broadly defining operation extremes. VTT's (Technical Research Centre of Finland Ltd) thermobalance was used for thermogravimetric analysis in order to investigate the reactivity and conversion of the wheat straw with and without additives. Test runs were carried out in steam, CO_2 and CO_2/Air-atmospheres at 750, 850, 900 and 950 ºC.

Residual ash from the thermobalance test runs was analysed by microscopy and the sintering degree was determined for each sample and condition. Scanning electron microscopy (SEM) and energy dispersive X-ray spectroscopy (EDS) were used to inspect the surface morphology and composition of ash.

Results show that using additives in wheat straw decreases sintering significantly regardless of the test conditions. Wheat straw with kaolin shows consistent decrease in reactivity in all test atmospheres. Kaolin forms a soft and brittle layer on residual ash and char inhibiting the reaction. In steam atmosphere test runs use of kaolin reduced reactivity significantly. Magnesium oxide seems to form a layer on residual ash only in steam atmosphere test runs decreasing reactivity slightly.

Keywords: gasification, ash, sintering, agricultural residue, feedstock, straw

CONTENT

ABBREVIATIONS AND TERMS

BFB	Bubbling fluidized-bed
CFB	Circulating fluidized-bed
CHN	Carbon, Hydrogen and Nitrogen
Char	Highly carbonaceous solid resulted from drying and pyrolysis of biomass
EDS	Energy Dispersive X-ray Spectroscopy
Empirical	Based on sensorial evidence
GHG	Greenhouse Gases
Pyrolysis	Physical volatilization of matter by heat degradation
SEM	Scanning Electron Microscopy
Sintering	Compacting and forming a solid mass of material by heat and/or pressure, without melting
TB	Thermobalance
TGA	Thermogravimetric analysis
VTT	VTT Technical Research Centre of Finland Ltd

1 INTRODUCTION

The use of renewable energy is imperative to reduce greenhouse gas emissions globally. Biomass has the biggest and most immediate impact towards this goal within Europe and in several regions of the world. (European Commission [EC] 2014) Bioenergy represented 5 % of the total energy production in Europe in 2010 (European Commission [EC] 2010), and current developments align well with the European Union targets for 2020 of renewable energy production reaching 20 % (European Commission [EC] 2015). Within this environment it is not only the use of biomass that matters but especially the responsible exploitation of biomass which minimizes environmental impact and delivers substantial emission savings. (EC 2014)

Biomass gasification can be deemed as an effective and sustainable process for the production of energy and chemicals in various scales around the globe (Kirkels & Verbong 2011). Smaller scale bioenergy production can have clear environmental advantages compared to large scales solutions when considering the whole life-cycle of biomass. Sourcing of biomass from third-countries with little regulation and transportation of feedstocks are matters of concern that are not applicable in smaller scales. (EC 2014) The small scale gasification of agricultural biomass wastes, or crop residues such as wheat straw, presents a case of clear economic and environmental advantage possibly reducing by over 90 % GHG emissions if compared to the use of fossil fuels (EC 2010).

This final thesis report presents the effect of magnesium oxide and kaolin on the ash sintering behaviour of wheat straw in the gasification process. Ash sintering and melt is a key issue originating from the feedstock properties. The use of additives in the feedstock has the specific purpose of reducing ash sintering allowing a wider operation range giving an even greater fuel flexibility to the gasification process. This work also supports deployment of bench-scale tests for the development of fixed-bed gasification solutions by broadly defining operation extremes with and without the use of additives. In order to investigate the reactivity and conversion of the wheat straw variants VTT's thermobalance was used. Ash sintering was analysed by microscopy, scanning electron microscopy (SEM) and energy dispersive X-ray spectroscopy (EDS).

2   BIOMASS AS GASIFICATION FEEDSTOCK

Biomass can be defined as the organic matter which is originated from living organisms or recently living organisms. The minutia of which different process derivatives can be still considered biomass is a matter of debate. (Basu 2010a) This gives biomass a huge scope, and herein the focus will be on process biomass feedstock within the European context. Given the nature of biomass as a greenhouse gas neutral resource and the direction of legislative policies, the use of renewable resources is imperative not only from a sustainable point-of-view, but also an economical one (EC 2014; Kirkels & Verbong 2011).

Biomass can be categorized using different criteria, such as end use, origin, energy content or timescale of growth. Biomasses can be classified as: virgin wood, energy crops, agricultural residues, food waste, industrial waste and co-products and manure (UK Biomass Energy Centre).

There are several minor and major challenges concerning feedstocks. Competition between food crops and energy crops, unavailable land, clearing of natural vegetation and the indirect impact of these on the global scale can affect GHG emissions negatively (European Environment Agency [EEA] 2013). Issues in gasification include the small scale use of biomass for local energy production, how to improve feedstock quality for the process by pre-treatment or selection, and furthermore transportation or scaling issues of biomass due to large distances between production and usage of biomass (State of Art Small Scale Gasification). Significant effort has been employed in characterizing and identifying issues arising from feedstock, especially concerning ash sintering (Moilanen 2006; Moilanen & Nasrullah 2011).

The overall best feedstocks in terms of process reliability and ease of implementation are dedicated wood crops, or virgin wood, given that such sources produce a negligible amount of ash. (Kirkels & Verbong 2011; Moilanen & Nasrullah 2011) On the other hand intensified demand for woody biomass could have a negative impact on the environment due to the sourcing from locations with unmanaged deforestation, implementation of dedicated crops which harm biodiversity in very large scales and the emissions caused by the aggregated logistics (EEA 2013). In this context the use of diversified biomass feedstocks in smaller scale gasification has potential for significant savings in GHG

emissions (Bocci et al. 2014). These diversified feedstocks are characteristic of agro-biomass and wood residues, from which the former includes wheat straw studied in this work. Economic advantages exist as demonstrated through commercialization of small scale solutions and political interest in using excess biomass for local energy production (EEA 2013).

3   GASIFICATION

3.1   Gasification

Gasification is the thermochemical conversion of carbonaceous compounds into a product gas, under high temperatures and oxygen-deficient environment, with an air-to-fuel equivalence ratio below 1. As opposed to combustion where the feedstock is oxidized giving heat, in gasification feedstock is reduced absorbing heat (Basu 2010a). The image below provides an overview of the biomass gasification process (figure 1).
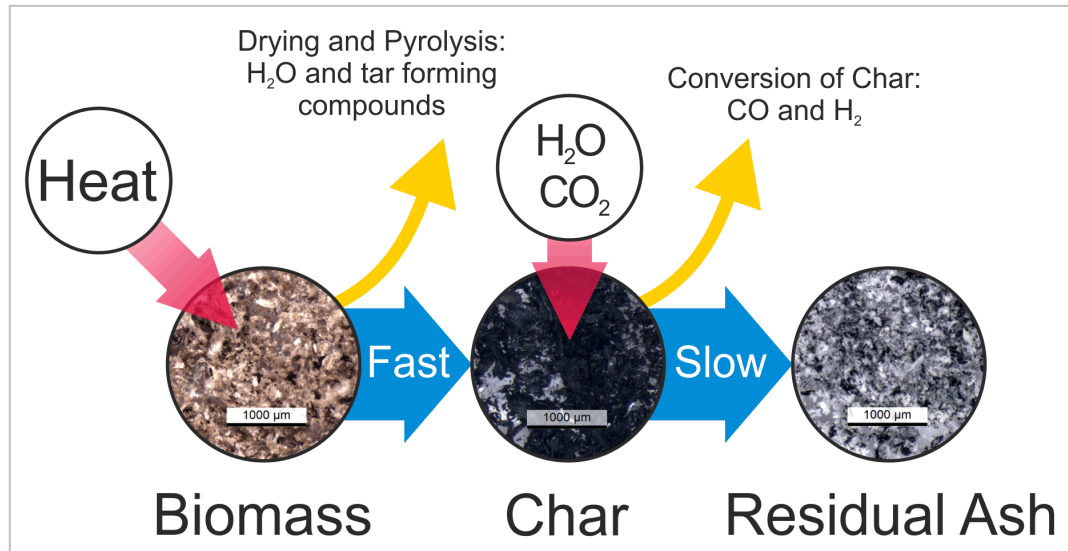

FIGURE 1. Simplified representation of biomass gasification

Biomass gasification is a fairly complex thermochemical process consisting of, in some cases, tens of reactions, thus its precise characterization and description can be a challenge. Biomass gasification can entail simultaneous reactions taking place at the gas phase, gas-solid interface and within the solid material. Main gasification reactions are shown in figure 2. The catalytic nature of ash affects the overall reactivity significantly and the properties of ash may vary between biomasses making it impossible to formulate a general model for reaction kinetics. Nevertheless, most aspects of biomass gasification are well understood and providing an overall description of the main chemical reactions and steps is rather straightforward. (Moilanen & Nasrullah 2011; Basu 2010b) For the scope of this work the relevant steps to present are the drying and pyrolysis of the biomass feedstock and the conversion of char into product gases.

Carbon Gasification (T > 700 $^{\circ}$C) $C + H_2O \rightarrow CO + H_2$ $C + CO_2 \rightarrow 2CO$ $C + 2H_2 \rightarrow CH_4$	Endothermic 11.3 MJ/kg C 14.2 MJ/kg C
Water-gas Shift (WGS) $CO + H_2O \leftrightarrow H_2 + CO_2$	Exothermic 2.8 MJ/kg C
Combustion $C + O_2 \rightarrow CO_2$	Exothermic 32.9 MJ/kg C

FIGURE 2. Main reactions of gasification (mod. Moilanen 2010)

During drying and pyrolysis biomass releases a large portion of its initial mass in the form of steam and volatile carbonaceous compounds (tar). These steps are very fast compared to the conversion of char. At insertion into the reactor biomass is exposed to very high temperatures exceeding water's critical vaporization temperature converting liquid water into steam which is quickly released from the biomass. The endothermic vaporization of water slows dramatically further heating of biomass until it is converted into steam. As the temperature of biomass rises pyrolysis strips biomass of its volatile carbonaceous compounds and the resulting tar can react further being converted to product gases or other compounds depending on the overall gasification process. It is important to note that in pyrolysis biomass is not undergoing any major chemical reactions, as opposed to combustion or proper gasification where oxidation and reduction are occurring respectively. The drying and pyrolysis steps overlap slightly but in all cases the former precedes the latter. The remaining mass of drying and pyrolysis is highly carbonaceous and is called char. (Basu 2010a)

Arguably at the core of the gasification process is the conversion of char into product gases. Due to the cellular structure of char (picture 1) the conversion reactions are mainly diffusion limited and reactions can take place within the cells. Thus in char conversion, preparation of the feedstock by grinding and the porosity have a significant effect on

reactivity. In practice, char conversion is the slowest step of gasification posing it as a limiting factor in the design of gasifiers.
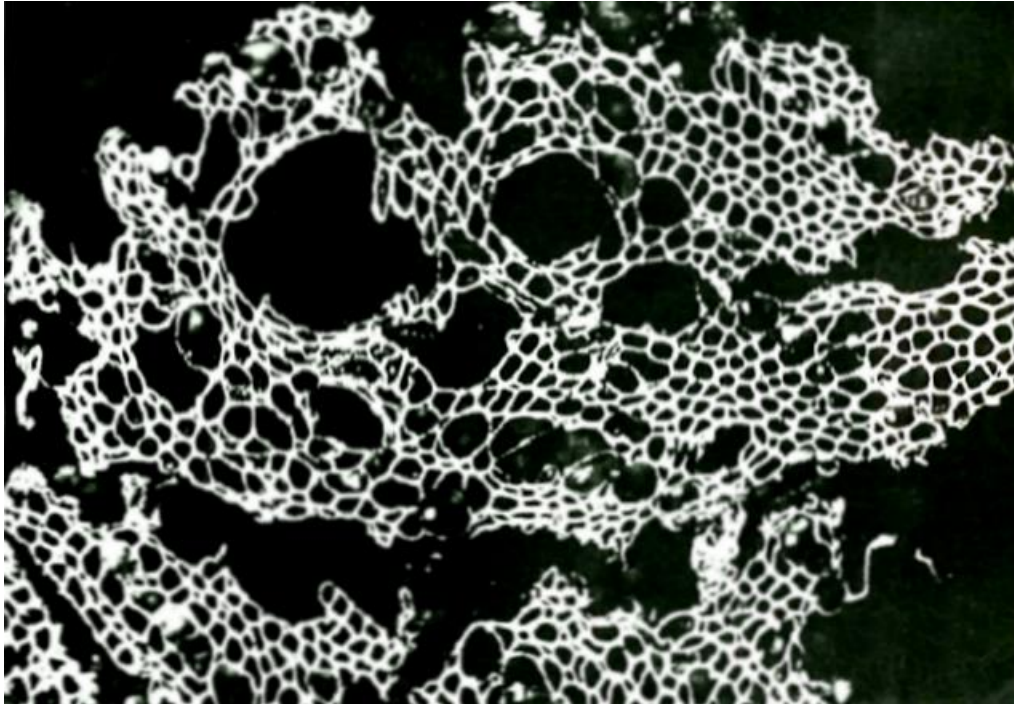
PICTURE 1. Cross-section of wood char showing its cellular structure (Moilanen 2010)

There are two main types of reactors in use for biomass gasification: fixed-bed and fluidized-bed reactors. Each solution has advantages and draw-backs, and they are generally targeted for specific demands.

3.2 Bubbling and Circulating Fluidized-Bed Gasifiers

Fluidized-bed reactors target medium to large scale gasification systems. These units require a sufficiently large input of feedstock and process gases to maintain proper operation. The most common implementations used in biomass gasification are the bubbling (BFB) and circulating (CFB) fluidized-bed reactors. (Moilanen & Nasrullah 2011) figure 3 provides a diagram of these reactor types. In fluidized-bed reactors all main steps of the process take place within the reaction bed and conversion can continue in the freeboard. In CFB gasifiers free-flowing particles are re-circulated through the bed achieving a higher conversion compared to BFB gasifiers. (Bocci et al. 2014)
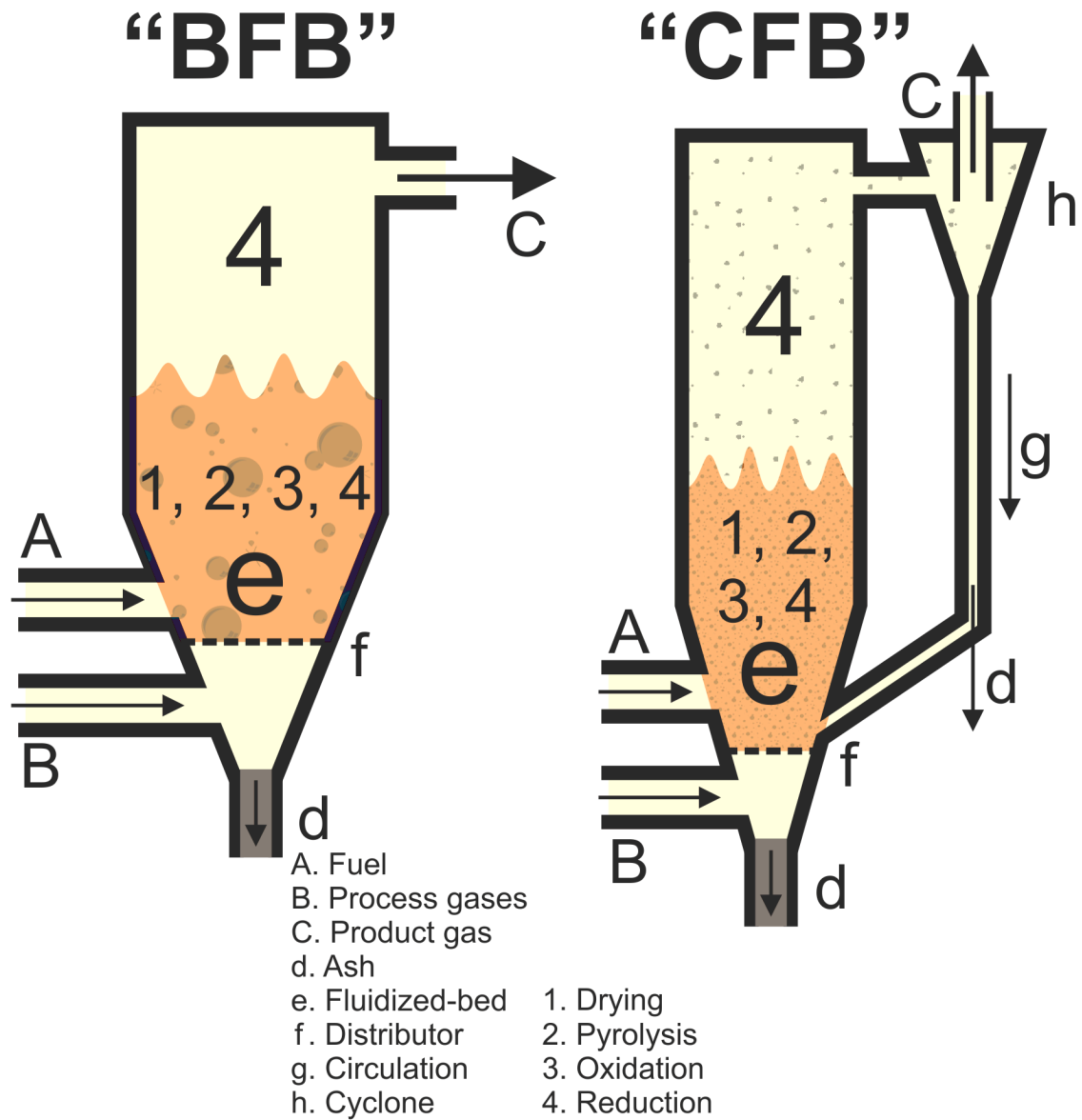
FIGURE 3. Bubbling "BFB" and Circulating "CFB" fluidized-bed gasifier diagrams with main steps and features (mod. Moilanen & Nasrullah 2011)

Fluidized-bed reactors are very agnostic to feedstock properties and they can be operated at higher temperatures than fixed-bed reactors without ash sintering issues for several problematic fuels. Main factors contributing to this are the bed attrition while the bed is fluidized, very homogeneous heat and mass transfer and lower maximum reaction temperatures. (Bocci et al. 2014; Moilanen & Nasrullah 2011)

3.3 Downdraft and Updraft Fixed-Bed Gasifiers

In fixed-bed gasification reaction steps take place within zones of varying temperature. The design of such gasifiers is fairly simple and they target small scale energy and heat production. Lack of attrition from a fixed-bed and accumulation of ash may cause sintering and slagging in these gasifiers. The reaction zones in a fixed-bed gasifier are the burning/oxidation, volatilization, reduction and pyrolysis zones as in figure 4.
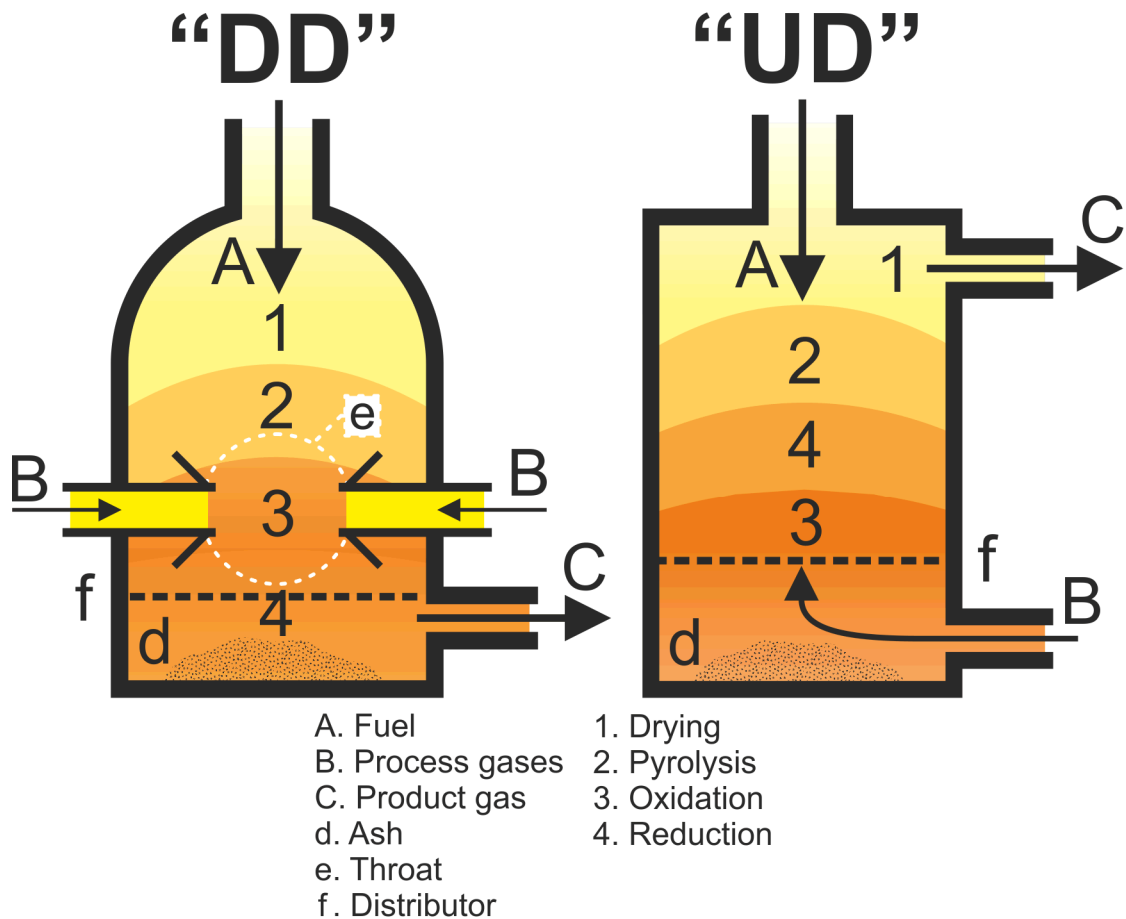

A. Fuel 1. Drying
B. Process gases 2. Pyrolysis
C. Product gas 3. Oxidation
d. Ash 4. Reduction
e. Throat
f. Distributor

FIGURE 4. Downdraft "DD" and Updraft "UD" gasifier diagrams with main steps and features (mod. Moilanen & Nasrullah 2011)

4 ADDITIVES AND ASH IN BIOMASS

The properties of ash in biomass is one of the most important factors for selecting appropriate gasification conditions. In biomass ash properties may vary greatly between feedstocks. Ash composition alone cannot predict sintering nor slagging on gasifiers, although it can be an indication of such behaviour (e.g. when ash has a high content of silicon and chlorine). (Skrifvars, Backman & Hupa 1998; Wilén, Moilanen & Kurkela 1996)

Ash plays a major role in biomass gasification because of its varied alkaline metal content. Alkaline earth metals such as potassium and calcium act catalytically on the active surface of char improving conversion and the reactivity of the feedstock. Perander et al. (2015) concluded that the reactivity increases linearly with the content of K or Ca in the feedstock. It is also noted that a dramatic fallout in the reactivity at the end of the reaction can be explained by the formation of layers of K_2CO_3 and $CaCO_3$ on the surface of char.

Additives in gasification have been used mainly in the reactor-bed (as bed material) to improve its catalytic properties (Pereira et al. 2012; Xu et al. 2010). These additives are applicable in fluidized-bed gasification, but not applied in fixed-bed gasification likely due to catalyst reforming issues. In fixed-bed gasification the use of additives is justified to improve ash slagging if the costs of implementation are low. Use of inexpensive additives already in the feedstock can prove to be an effective method in improving the feedstock flexibility of fixed-bed gasifiers.

5 EXPERIMENTAL PART

5.1 Feedstock and Additives

Feedstocks used in this work were wheat straw as such grounded to below 1 mm particle size (picture 1) and its mixture with magnesium oxide (MgO) and with kaolin. The feedstock mixtures were prepared by adding to pure wheat straw 4,5 wt.-% MgO or kaolin. Kaolin is a naturally occurring mineral (kaolinite) composed of aluminium oxide, silicon oxide and water with a formula based on oxides equal to $Al_2O_3 \cdot 2SiO_2 \cdot 2H_2O$. Feedstock analysis include moisture content, ash content, CHN and ash composition. Complete analysis tables are provided in Appendix 1. Note that ash composition of wheat straw with magnesium oxide has been calculated based on the ash composition of pure wheat straw and the amount of added MgO.
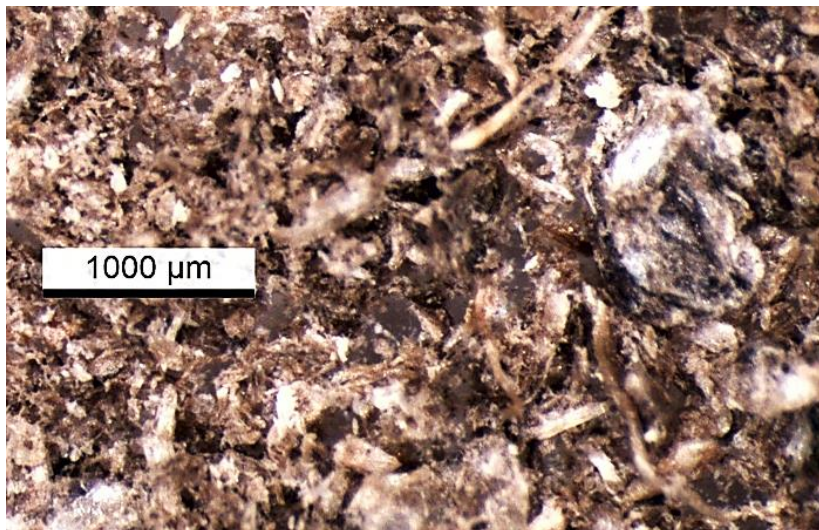
PICTURE 2. Photograph of pure wheat straw sample

5.2 Thermobalance (Thermogravimetric Analysis)

The pressurized thermobalance (figure 5) at VTT is a specialized test rig for studying the reaction kinetics of thermochemical processes. Process gases (e.g. steam, air or CO_2) are fed into the reactor at a chosen temperature and pressure simulating different operation conditions. Temperatures in the reactor can be a maximum of 1000 °C while pressures of up to 100 bars are possible. Sample sizes vary from 30-120 milligram, up to 1000 mg when operating the microbalance on lower precision mode.
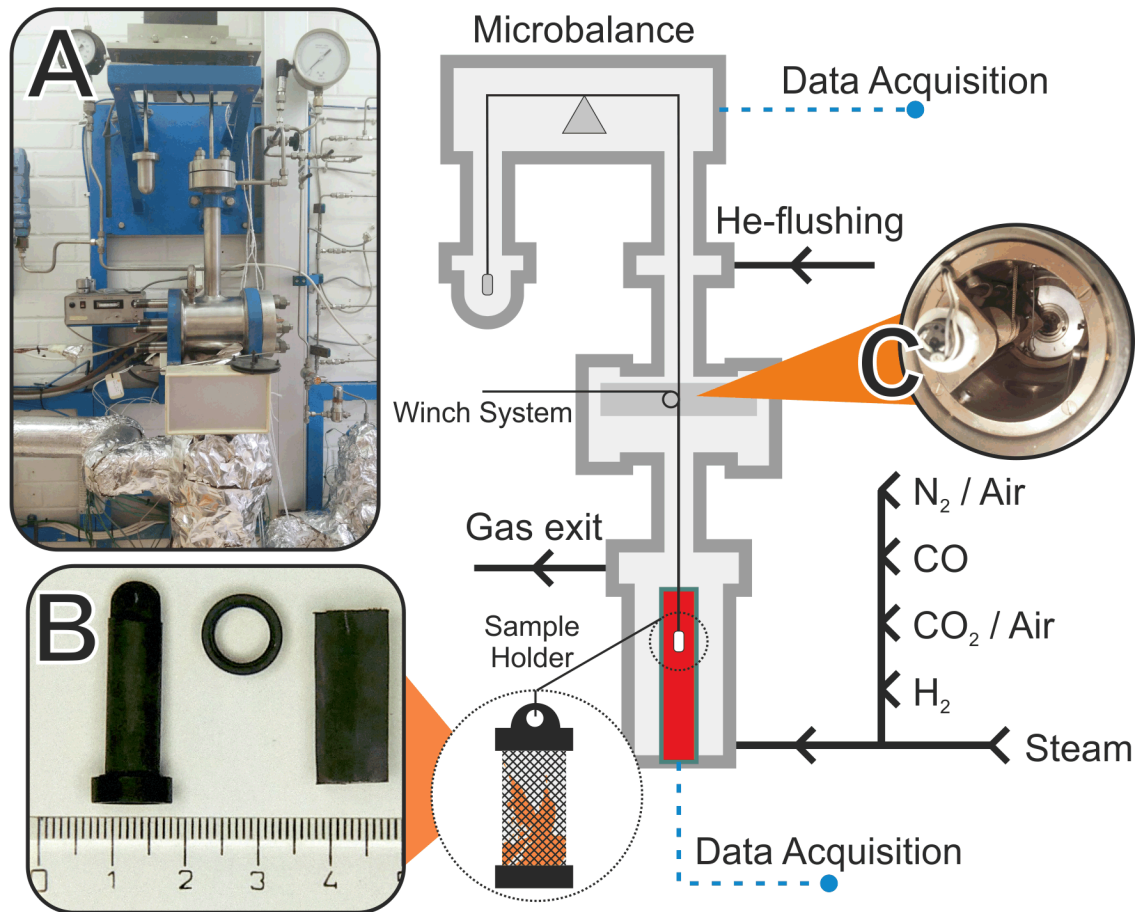
FIGURE 5. Thermobalance diagram; Pictures: A –Thermobalance, B – Sample holder, C – Winch system and sample chamber interior

In the thermogravimetric analysis (TGA) a highly precise microbalance with a continuous buoyance effect correction measures the mass of the sample during the reaction. To protect the sample from reacting prematurely the sample chamber is cooled and helium is fed at twice the combined flow rate of other gases. Cooling and helium also shield the sample chamber and microbalance from the process gases.

For each TGA-run feedstock is distributed homogeneously to the sample holder. The sample is placed in the hook of the winch system and closed inside the sample chamber. The reactor is heated to the target temperature and helium is fed to the system. Process gases are allowed to flow for 10 min (15 min if steam is used) to stabilize the gas composition. The sample is lowered rapidly into the reaction zone. In the reaction zone the sample holder is released from the winch system loading the microbalance (measurement starts). Drying and pyrolysis begin even before the sample has been lowered completely. Raw data from the microbalance (figure 6) is monitored until it stabilizes, indicating no further reaction, and the test can be stopped. In rare cases ash

continues to degrade very slowly, and it is at the operator's discretion to stop the test or continue until all possible reactions have finished. Equation (1) shows the calculation of conversion, and equation (2) the calculation of instantaneous reaction rate, conversion and reactivity are calculated from the ash-free mass. Residual mass as either partially unreacted sample or ash, is weighted and can be further studied by microscopy, SEM and EDS.
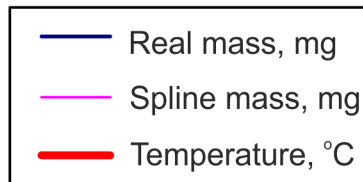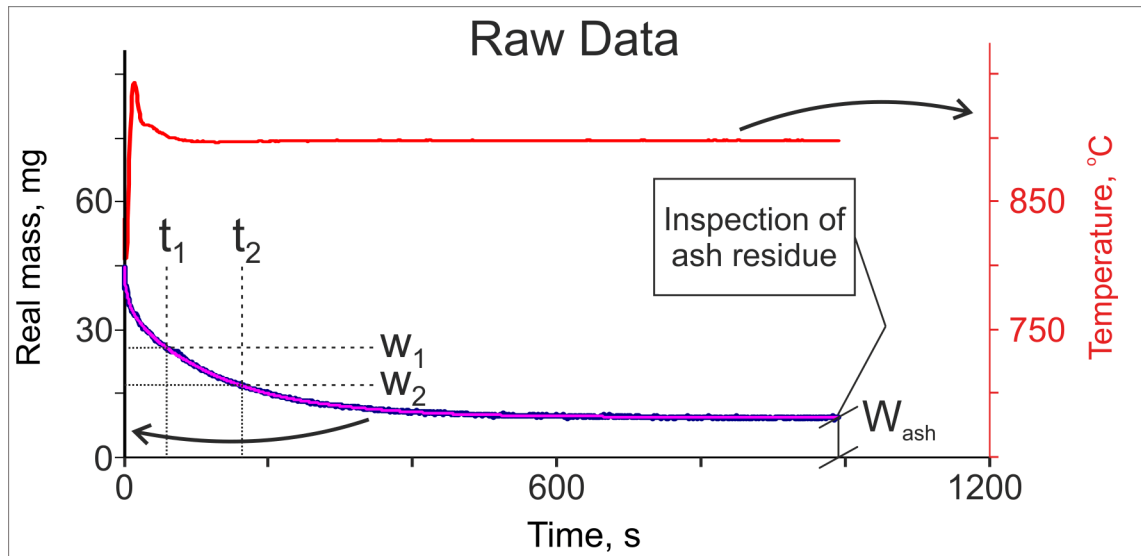
(1) Conversion

$$X, \% = 100\ [\%] * \frac{W_{sample}\ [mg] - W_2\ [mg]}{W_{sample}\ [mg] - W_{ash}\ [mg]}$$

(2) Instantaneous Reaction Rate

$$r'', \% / min = 100\ [\%] * 60\ [s / min] * \frac{W_1\ [mg] - W_2\ [mg]}{(W_2\ [mg] - W_{ash}\ [mg]\ ) * (t_2\ [s] - t_1\ [s])}$$

FIGURE 6. Raw data obtained from thermobalance with smoothed curve (spline); equations for conversion (1) and instantaneous rate (2)

Typical reactivity profiles calculated from the raw data are shown in figure 7. Reactivity can increase, decrease or go through a maximum depending on the fuel and the test conditions.
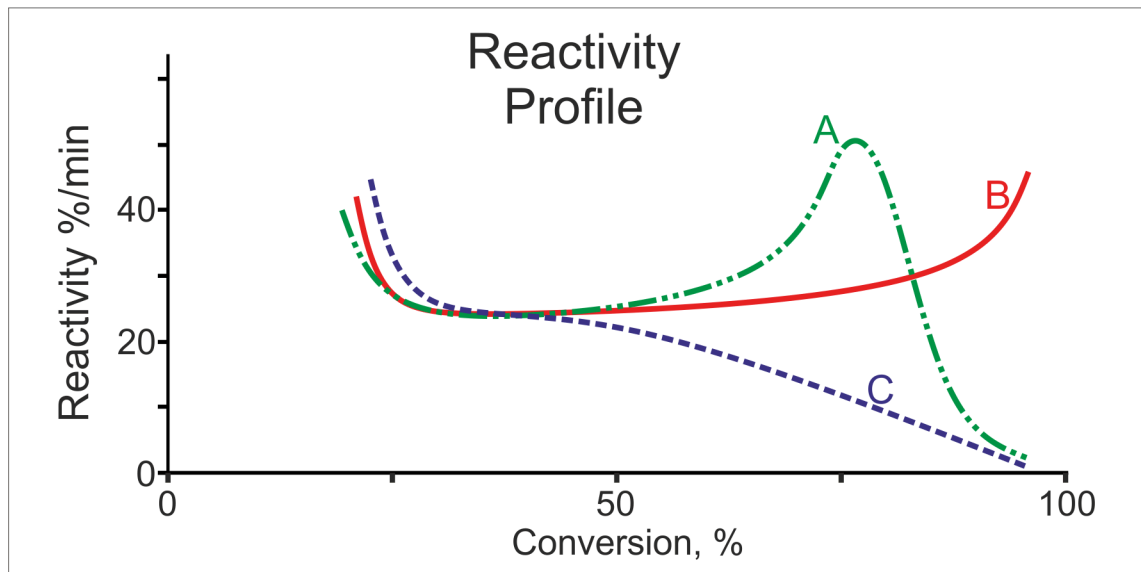

FIGURE 7. Typical reactivity profiles: A – reactivity has a maximum, B – increasing reactivity and C – decreasing reactivity

5.3   Test-Matrix

The test-matrix was designed to represent roughly the conditions in a fixed-bed gasifier where the issues caused by sintering are more pronounced if compared to fluidized-bed gasifiers. All the test points conducted in this work were done at atmospheric pressure. In the mixture of CO_2 and air (CO_2/Air-mixture) the partial pressure of the gases was 75 % and 25 % respectively. Table 1 provides a summary of the test points carried out in this work.

Tests using CO_2/Air-mixture represent the conditions in the oxidation zone with higher temperatures and very fast reactions. Tests at lower temperatures with additives are equivalent to conditions found in the reduction zone. The reactivity profiles can be compared to examine the effects of additives on the kinetic behaviour of the feedstock.

TABLE 1. Test-matrix of wheat straw thermobalance runs at different temperatures with and without additives

Gas atmosphere		H_2O			CO_2	CO_2/Air		
T [^{o}C]	Additive	-	Kaolin	MgO	-	-	Kaolin	MgO
750		X	-	-	-	-	-	-
850		X	X	X	X	X	X	X
900		X	-	-	X	X	X	X
950		-	-	-	-	X	X	X

5.4 Ash Sintering Microscopy

The determination of ash sintering in microscopy is an empirical process and several factors influence the sintering degree of the sample. In this work a LEICA MZ12 stereoscopic microscope with a DCF LEICA digital camera is used. Visually the most important aspects are the presence and size of melt particles, the bridging of ash particles caused by melt, the overall shine of ash and the formation of large networked structures. Partially reacted, or unreacted, char particles usually remain fairly large, thus size alone is a poor indicator of sintering. Reacted non-sintered particles can be crushed easily into very fine particles as in figure 8.

1 mm

FIGURE 8. VTT's sintering classification from left to right O, *, **, *** (mod. from Moilanen 2006)

This classification system has been developed at VTT and the sintering degrees are detailed further in table 2, explaining the basis for each category (Moilanen 2006).

TABLE 2. Sintering classification system (Moilanen 2006; Moilanen & Nasrullah 2011)

Degree	Explanation
O	No sintering, very fine particles can easily be crushed into powder. There are virtually no structures in ash, nor fused melt. Molten particles may appear in sample but they are not fused with ash.
*	Slight sintering, fine-medium sized particles, structures can be seen, particles can be crushed into powder. Molten particles present, very slight fusing.
**	Significant sintering, medium sized particles, crushing particles is challenging, a clear crackling sound is produced, obvious structures and networks of ash present. Molten particles are present in significant quantity, obvious fused ash and melt.
***	Completely sintered or molten, particles cannot be crushed manually, particle size is fairly large, ash cannot be visually separated from melt. Melt appears either fused together as a blob or in localized fairly large particles.
()	Parenthesis present a more refined scale. Thus a grading of **(*) would represent the presence of significant sintering closely trailing complete sintering of ash, and (*) would represent a sample with almost no sintering, or sintering that is difficult to confirm.

The sintering can further be confirmed by the distinctive crackling sound produced when sintered particles are broken. It is important to recognize that different feedstocks present a visually different scenario, thus comparing sintering and ash melt across different feedstocks is not always straightforward. A certain degree of subjectivity is always present and specific deterministic methods for sintering analysis are not currently available. Therefore, results concerning sintering should be read carefully and the microscopy photographs are of utmost importance in interpreting the results correctly. The analysis here-in follows VTT's internal framework as provided first in (Wilén et al. 1996).

5.5   SEM & EDS Analysis

Scanning electron microscope (SEM) in conjunction with energy dispersive X-ray spectroscopy (EDS) analysis is used in a subset of samples to provide a much more accurate observation of the ash morphology and qualitative composition of the ash surface. The use of SEM is essential to observe structures on the very small scales pointing to the presence of unreacted char particles, formation of melt (drops) and hardened shells, presence of impurities, which can be confirmed with EDS. In addition, EDS mapping of the surface can inform on the distribution of specific elements and their concentrations.

6 RESULTS

6.1 Thermobalance

Test runs which showed unexpected behaviour were repeated for verification purposes and the most consistent result is used. Notice that graphs presented here were drawn using the wt.-% of ash residue obtained from the TGA runs (table 3).

TABLE 3. Ash content [wt.-%] of sample as determined from TGA run residues

Gas atmosphere		H_2O			CO_2	CO_2/Air		
T [^{o}C]	Additive	-	Kaolin	MgO	-	-	Kaolin	MgO
750		8.46						
850		6.17	7.14	8.04	5.51	5.94	7.93	8.19
		5.58			5.82			
900		5.96			5.63	6.05	7.97	8.13
950						6.22	7.40	8.01
						6.28		
						5.63		

Numerical data of the reactivity at 85, 90 and 95 % fuel conversion stage for each sample is given in table 4. Notice that reactivity in test runs with CO_2/Air-atmosphere is very high and these values only get exacerbated at higher conversions, thus a big numerical difference (i.e. 30-40 %) has little effect on conversion times presented in table 5.

TABLE 4. Reactivity at 85 %, 90 % and 95 % fuel conversion stage [% / min]

Gas atmosphere		H_2O			CO_2	CO_2/Air		
T [^{o}C]	Additive	-	Kaolin	MgO	-	-	Kaolin	MgO
750	At 85%	15						
	At 90%	2.6						
	At 95%	1.5						
850	At 85%	69	47	50	65	147	140	159
	At 90%	34	26	30	22	160	145	164
	At 95%	22	11	18	24	255	232	276
900	At 85%	89			59	182	154	177
	At 90%	88			50	210	186	205
	At 95%	69			53	303	278	329
950	At 85%					191	195	214
	At 90%					249	246	283
	At 95%					375	345	433

TABLE 5. Time needed until 99 % fuel conversion is reached [min]

Gas atmosphere		H_2O			CO_2	CO_2/Air		
T [^{o}C]	Additive	-	Kaolin	MgO	-	-	Kaolin	MgO
750		> 110						
850		13.2	30.2	16.5	10.8	1.55	1.68	1.55
900		4.8			5.8	1.28	1.42	1.25
950						1.13	1.14	1.02

Figure 9-11 compare the reactivity of pure wheat straw and doped wheat straw at different temperatures in CO_2/Air-atmosphere, while figure 12-14 compare conversion rates in these conditions. Results show that at 900 and 950 ^{o}C straw with MgO has the best overall reactivity, with a few seconds lower fuel conversion times, a very small difference for practical applications. Kaolin has a more pronounced fallout in reactivity at both 850 and 900 ^{o}C, but at 950 ^{o}C pure wheat straw has a more pronounced fallout in reactivity. Conversion of pure wheat straw struggles to reach 100 % at 900 ^{o}C, wheat straw with MgO shows similar behaviour at 950 ^{o}C, this could be caused by some residual carbon remaining in a site of slow diffusion.
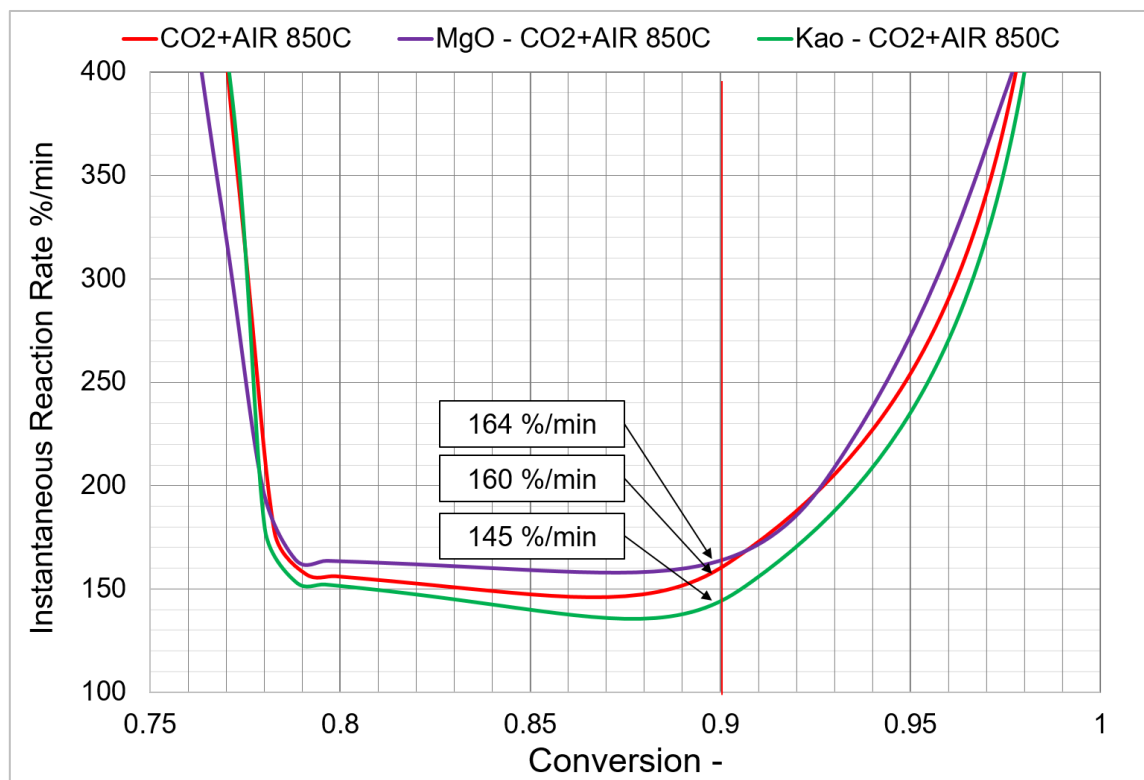
FIGURE 9. Reactivity profiles in CO_2/Air-atmosphere at 850 ^{o}C
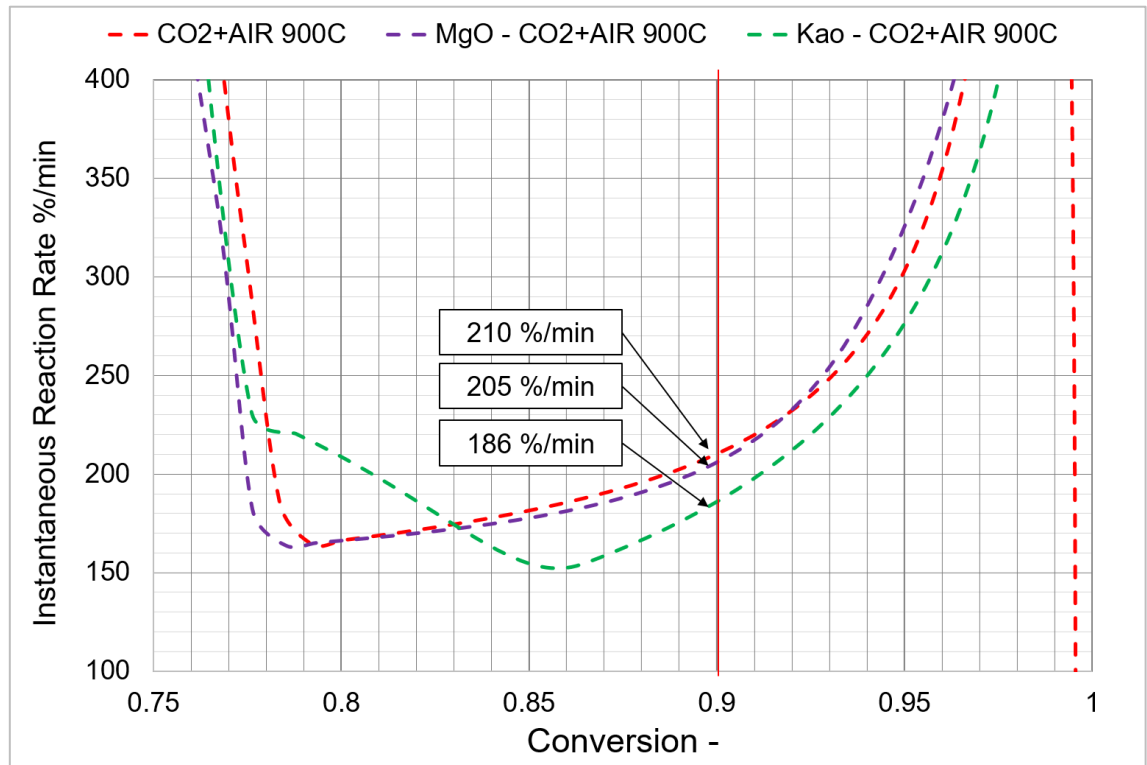
FIGURE 10. Reactivity profiles in CO_2/Air-atmosphere at 900 ºC
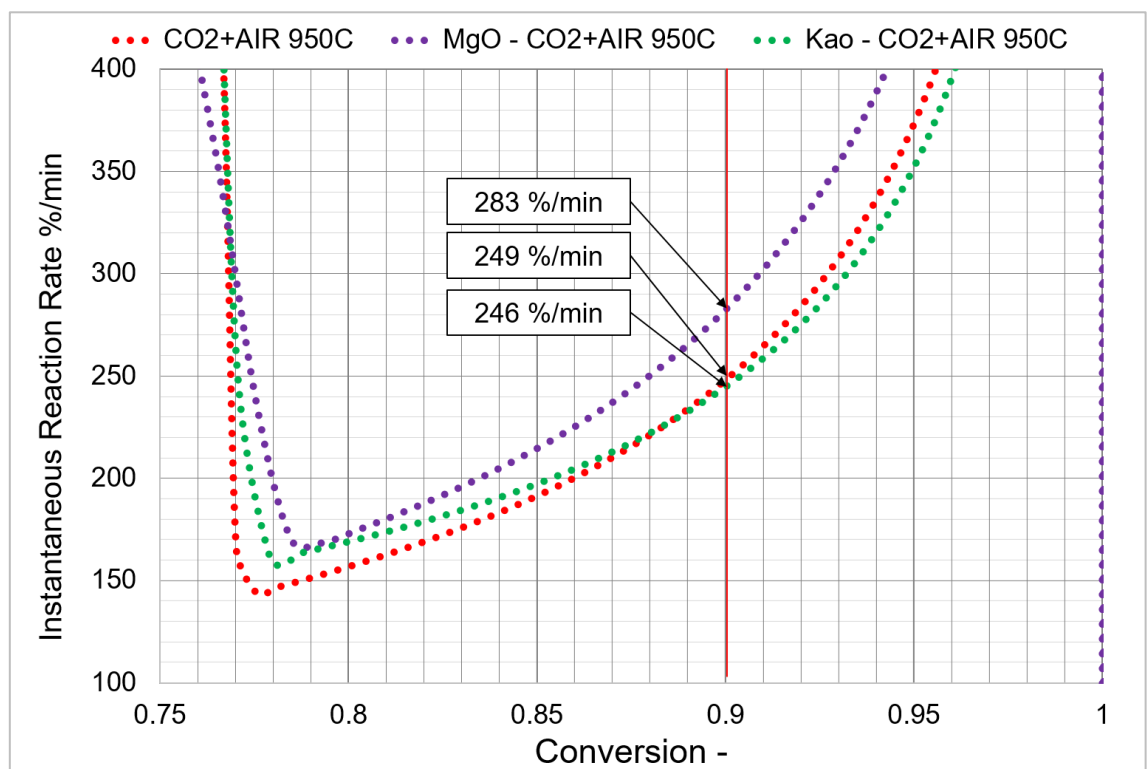
FIGURE 11. Reactivity profiles in CO_2/Air-atmosphere at 950 ºC
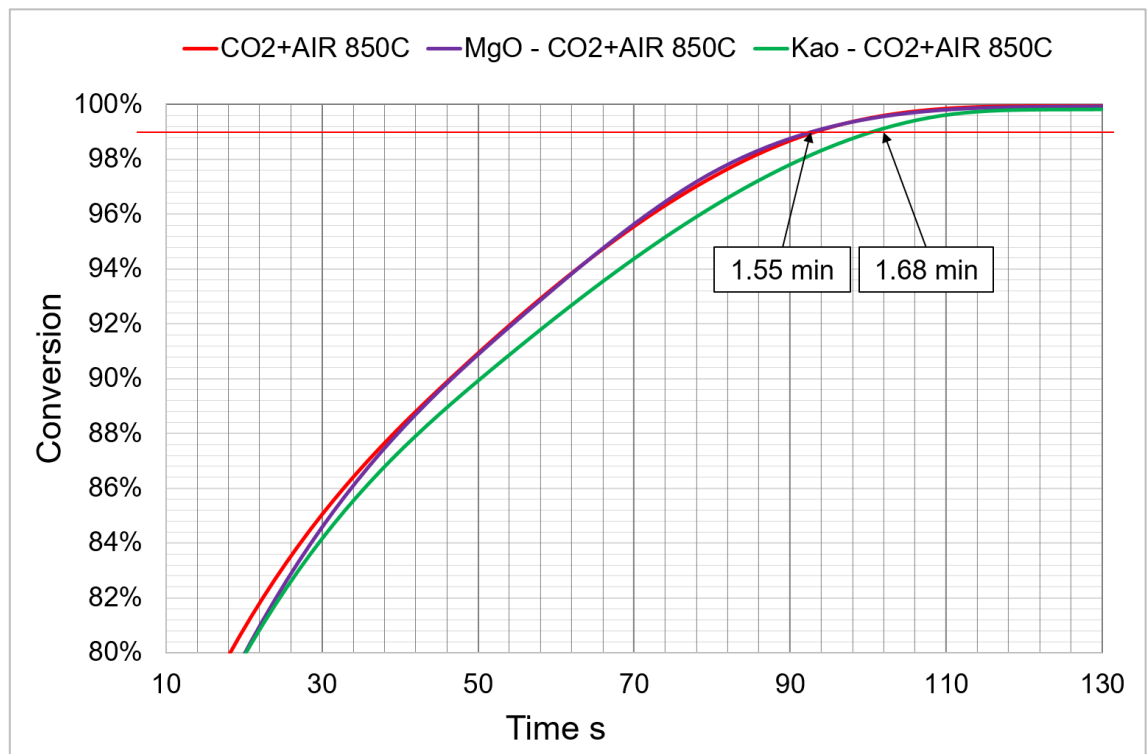
FIGURE 12. Conversion times in CO_2/Air-atmosphere at 850 °C
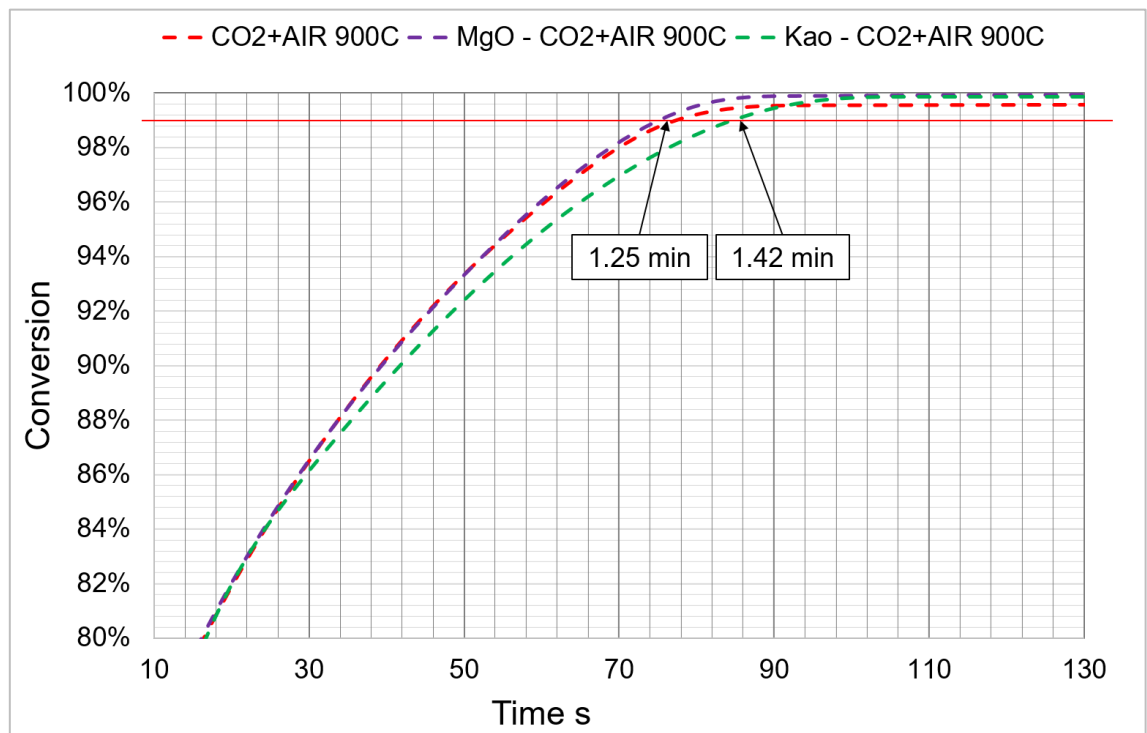
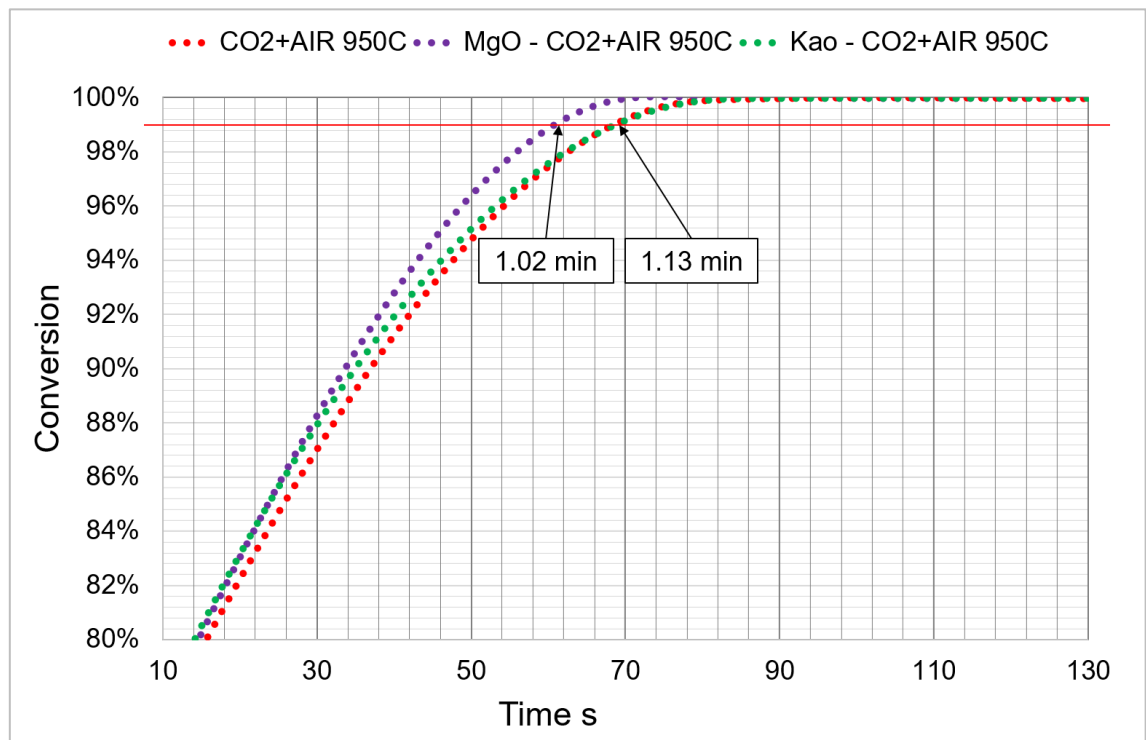FIGURE 13. Conversion times in CO_2/Air-atmosphere at 900 °C

FIGURE 14. Conversion times in CO_2/Air-atmosphere at 950 °C

Reactivity for both steam and CO_2 gasification are of similar magnitudes and comparable, but each presents a unique reactivity profile and disparate conversion time as shown in figure 15 and figure 16. Steam gasification reactivity decreases in steps at two distinct points in each run. Even though steam gasification is faster at first, CO_2 gasification finishes earlier in 850 °C test runs.
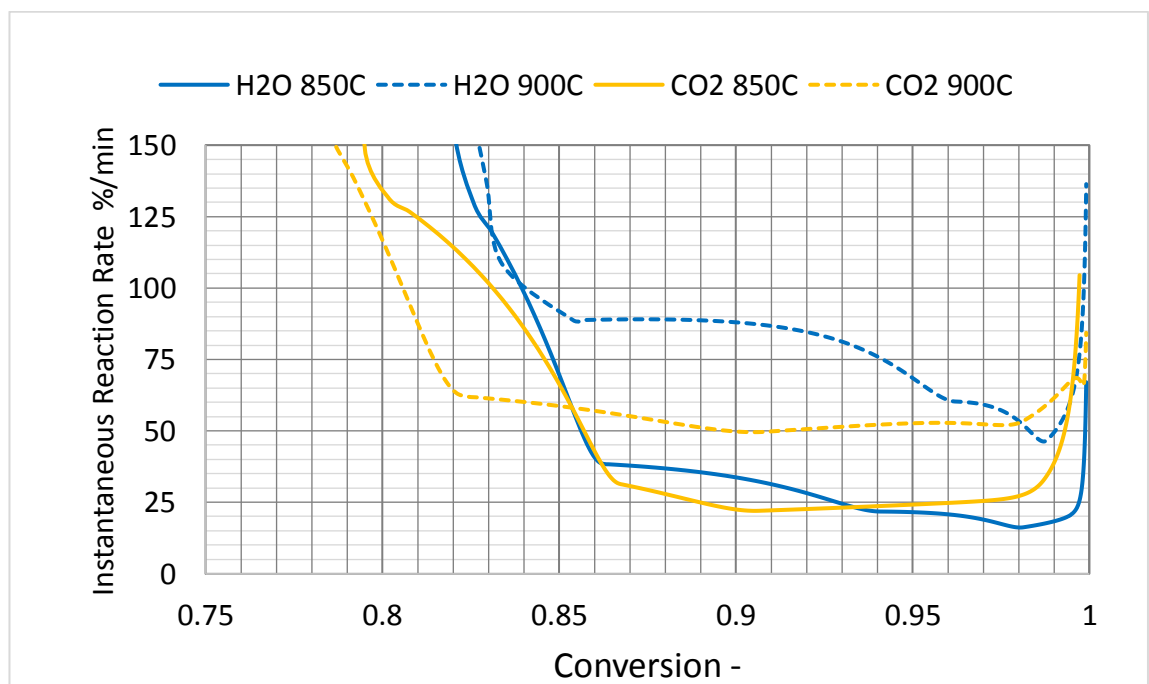
FIGURE 15. Reactivity profiles in steam and CO_2 atmospheres compared at 850 and 900 °C
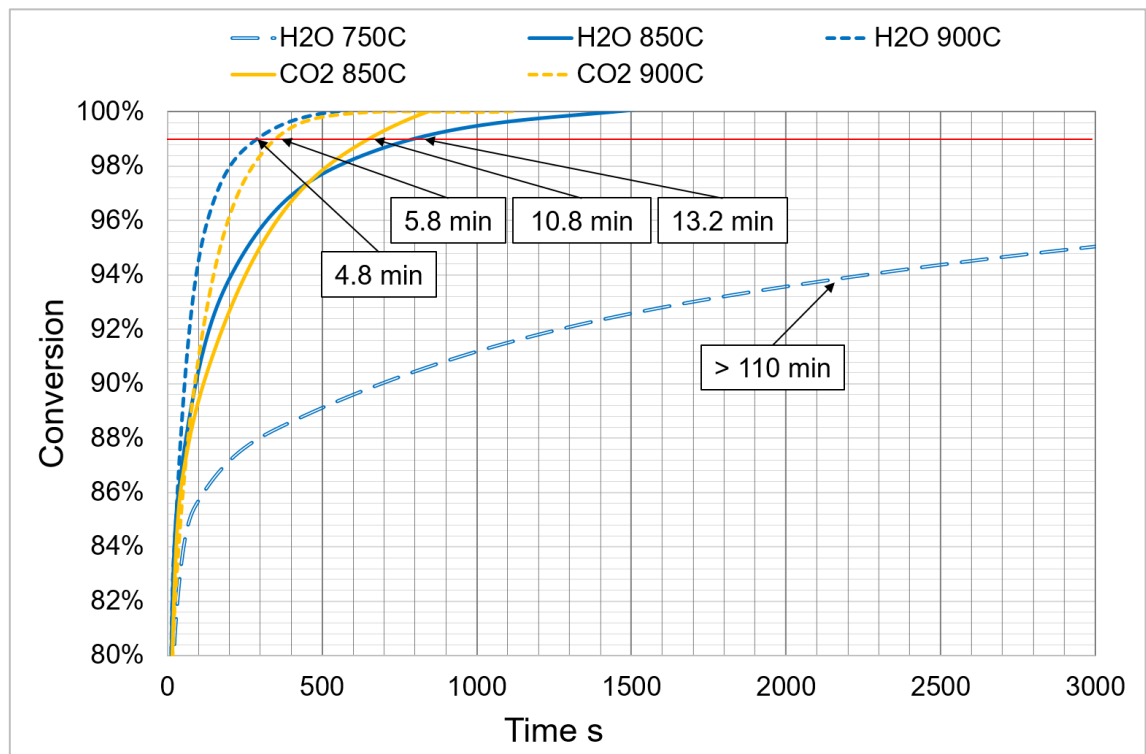
FIGURE 16. Conversion times in steam and CO_2 atmospheres compared at 850 and 900 °C

Results of TGA runs with steam and with additives show a somewhat different trend compared to runs in CO_2/Air-atmosphere (figure 17-18). Addition of magnesium oxide decreases reactivity somewhat, resulting in a conversion time difference of over 3 min compared to pure wheat straw. There is an increase of 17 min in conversion time when kaolin was used, this is due to low reactivity specially after the 90 % fuel conversion stage. As expected, all reactivity profiles exhibit steps in their reactivity. Reactivity at 750 °C is almost stagnant and achieving total conversion would take over 2 hours.
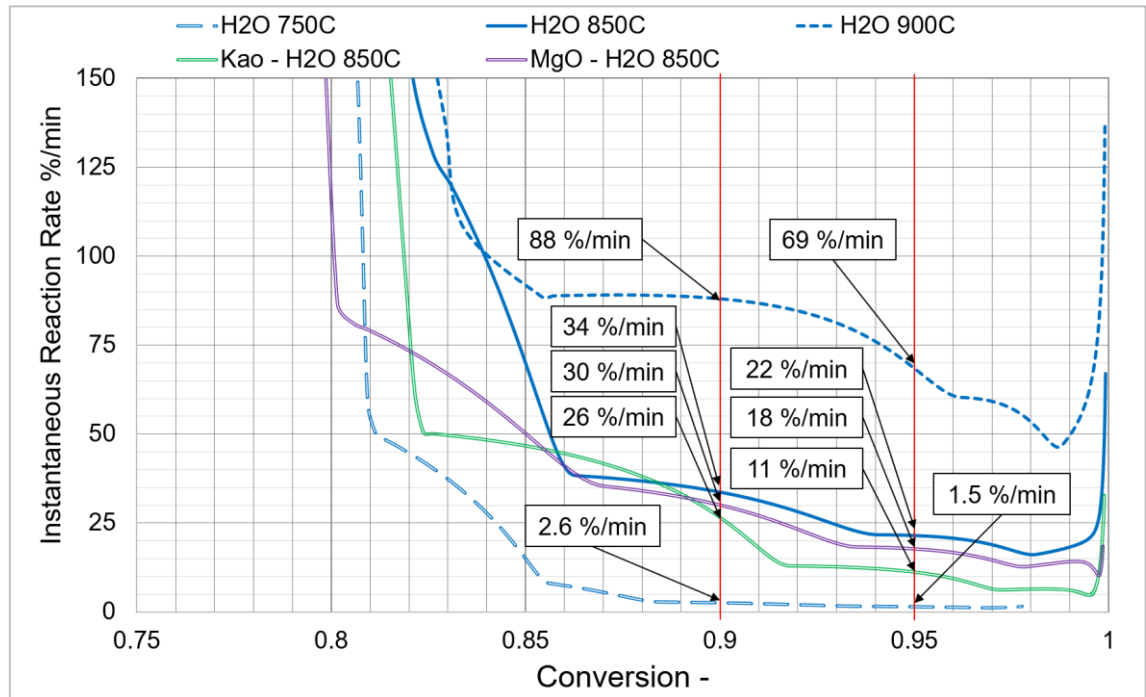
FIGURE 17. Reactivity profiles in steam atmosphere compared at 750, 850 and 900 oC
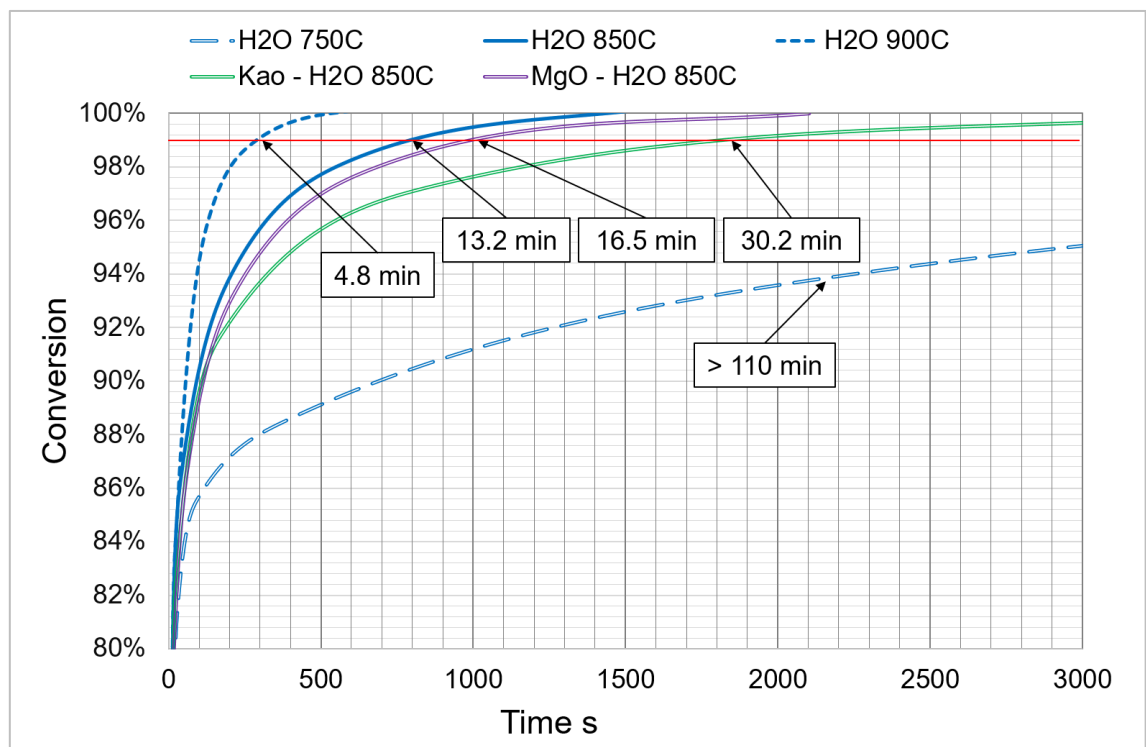
FIGURE 18. Conversion times in steam atmosphere compared at 750, 850 and 900 ºC

6.2 Microscopy

In Appendix 2 a full listing of all the samples and their sintering degree is provided. For a quick reference table 6 provides a summary of the sintering degree of all samples. Results show that sintering is more pronounced in the test runs with steam and CO_2 gasification. The test runs with additives have a much lower sintering tendency than comparable tests runs with pure wheat straw.

TABLE 6. Summary of sintering degree of all samples

Gas atmosphere		H₂O			CO₂	CO₂/Air		
T [°C]	Additive	-	Kaolin	MgO	-	-	Kaolin	MgO
750		O						
850		*(*)	(*)	(*)	*(*)	*	(*)	O, mp
		*(*)			*(*)			
900		***			**	*(*)	(*)	O, mp
950		mp = molten particles				**	(*)	O, mp
						**(*)		
						**		
						**		

Wheat straw ash has a black colour, and as ash sintering progresses towards melt it goes through a grey coloration. All pictures were taken from a location in the ash residue that represented best the sample right after the reaction. During inspection of the samples sintered structures were mostly crushed.

Ash residue from test runs in CO₂/Air-atmosphere at 950 ºC

In picture 3 ash from pure wheat straw exhibited strong sintering **, but not total fusing of the ash into a solid slag. Most of the sample particles had sintered to over 1 mm in size, with significant amount of smaller molten particles.
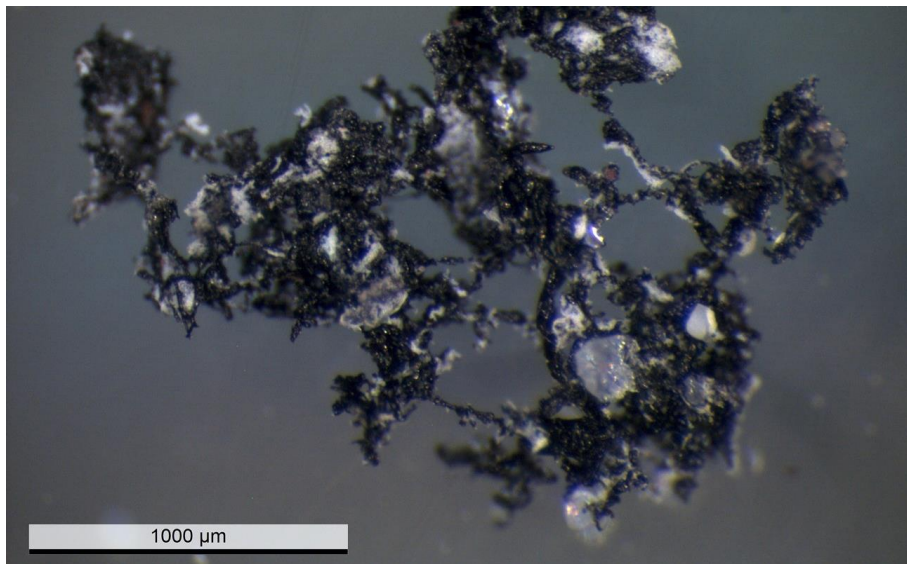
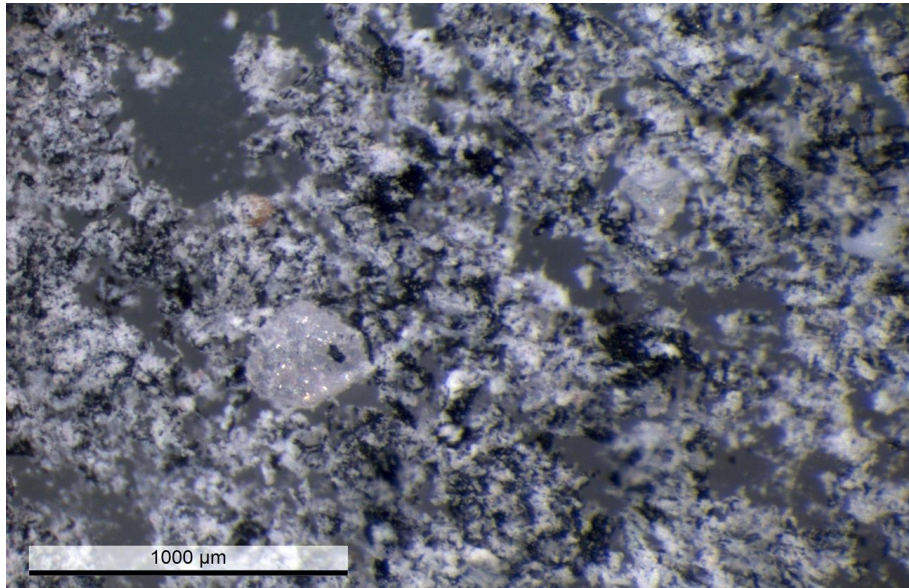PICTURE 3. Wheat straw ash, CO_2/Air-atmosphere gasification at 950 $^{\circ}$C, sintered **

In picture 4 ash of wheat straw with kaolin has almost no sintering (*). Very little inter-particle sintering is present, particles have a fairly elongated shape and big size. Molten crystals are present though very translucent and not fused with ash. Particles are crushed easily having a soft sound, indicating a very-low sintering degree. The contrast between uncovered particles and particles covered with kaolin is fairly clear, indicating possible shielding of char by kaolin, which could lead to larger residual particles.
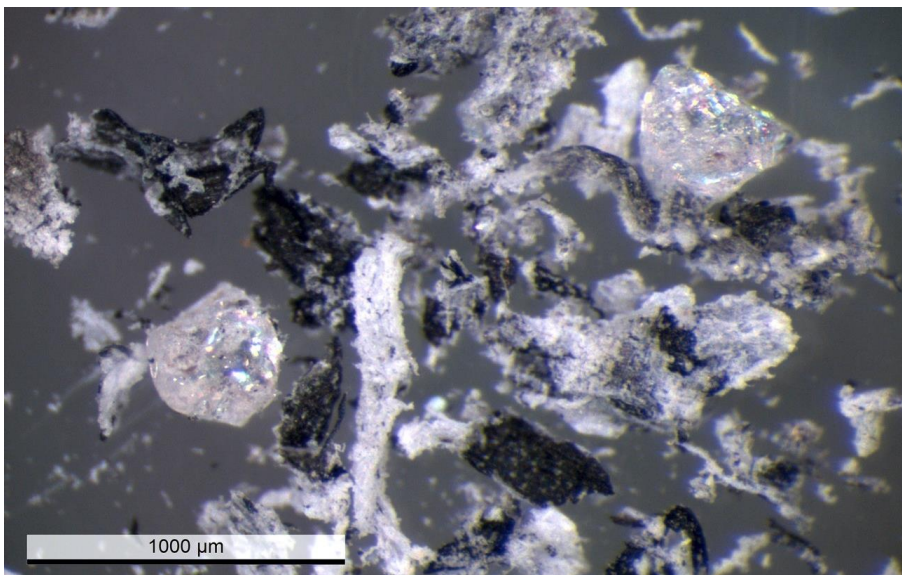
PICTURE 4. Kaolin doped wheat straw ash, CO_2/Air-atmosphere gasification at 950 $^{\circ}$C, sintered (*)

Ash from magnesium oxide doped wheat straw exhibits no sintering O, but molten particles are present in the ash. Residual particles are very fine, and although magnesium

oxide can be visually distinguished from ash, it is distributed homogeneously on the whole sample, see picture 5.

PICTURE 5. MgO doped wheat straw ash, CO_2/Air-atmosphere gasification at 950 ºC, sintered O, with molten particles

Ash residue from test runs in steam atmosphere at 850 ºC

In picture 6 ash from pure wheat straw exhibited a sintering degree of *(*). Melt particles are present, some of which are fused contributing to this classification.
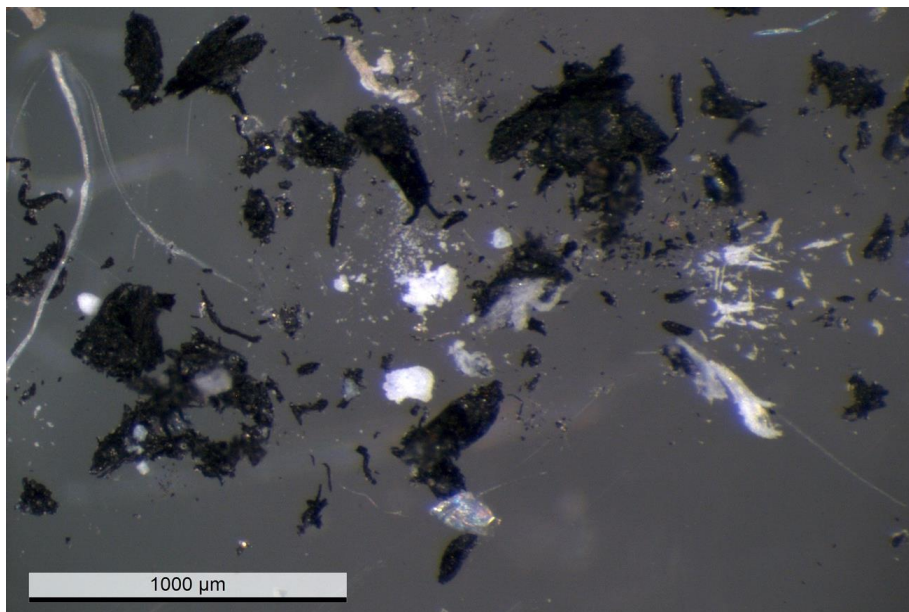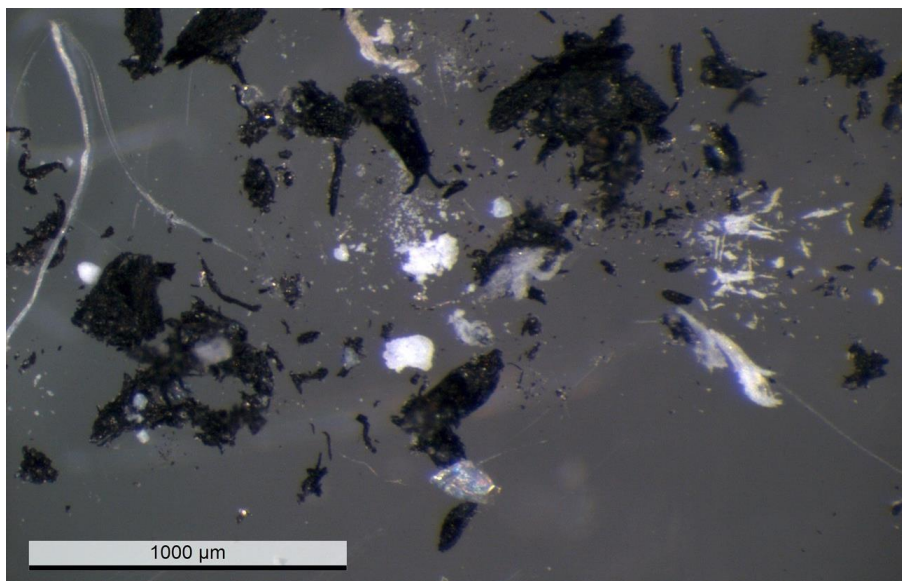

PICTURE 6. Wheat straw ash, steam gasification at 850 ºC, sintered *(*)

Ash in picture 7 exhibits very weak sintering (*). Little inter-particle sintering is present, but particles are slightly hardened. Very small molten particles are present. In steam test runs the overall size of the particles is significantly smaller than in the test run in CO_2/Air-atmosphere at 950 °C.
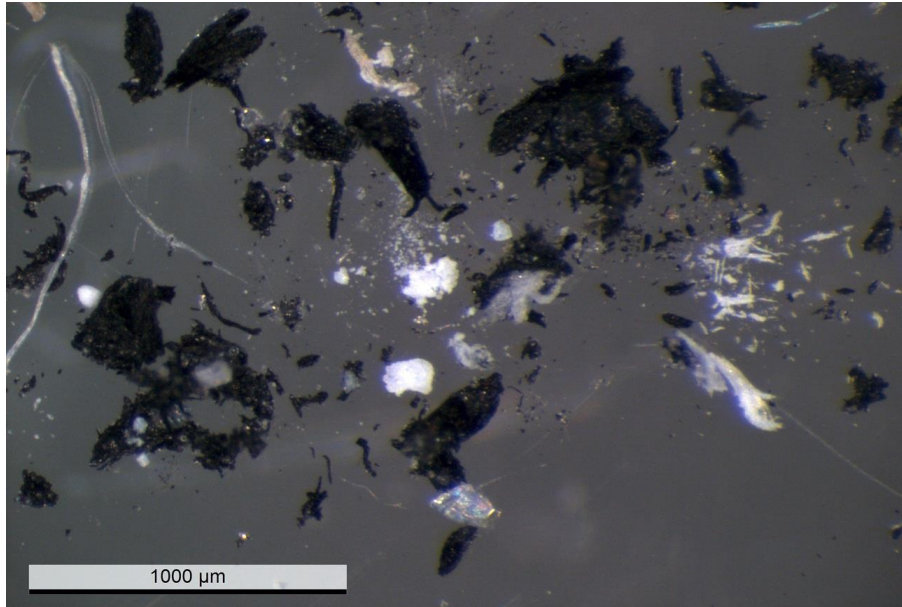
PICTURE 7. Kaolin doped wheat straw ash, steam gasification at 850 °C, sintered (*)

Compared to the test in CO_2/Air-atmosphere, wheat straw with magnesium oxide behaves very differently in steam gasification at a lower temperature. In picture 8 wheat straw with magnesium oxide has a sintering degree of (*). Magnesium oxide seems to be covering particles in a similar way as kaolin. Larger particles seem to be covered with smooth layers of MgO. The ash is softer than kaolin doped ash.


PICTURE 8. MgO doped wheat straw ash, steam gasification at 850 °C, sintered (*)

6.3   SEM & EDS Analysis

Morphology and surface composition of the ash residue samples was studied using SEM and EDS. Morphology of kaolin and melt on the surface of ash is presented in picture 9 and picture 10. Melt has a liquid appearance on the surface of ash, while kaolin maintains a more aggregated and granular shape. Areas of both high aluminium and silicon content are indicative of kaolin, while areas having mostly silicon are commonly representative of ash components interacting with silicates forming a low melting point mixture.
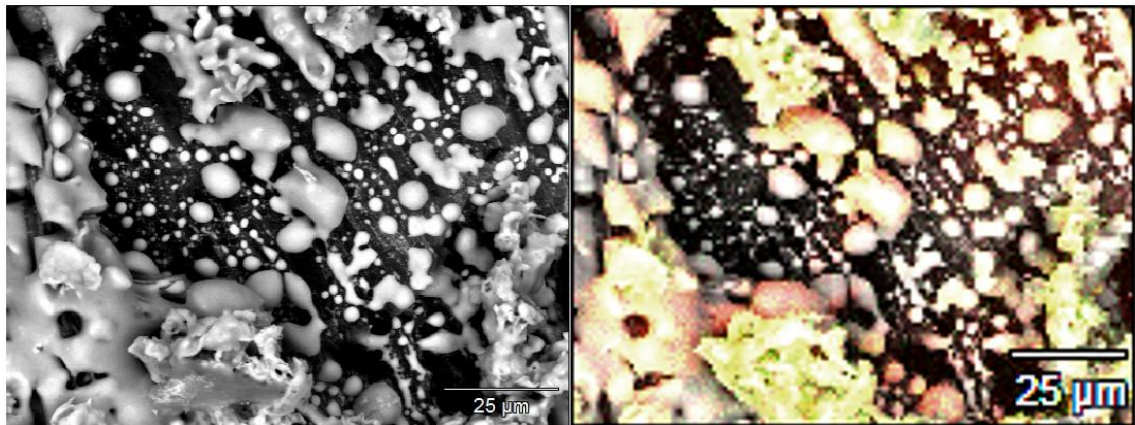
PICTURE 9. SEM picture (left) and EDS mapping of Si (red tint) and Al (green tint) over original (right); Wheat straw with kaolin from steam atmosphere at 850 $^{\circ}$C
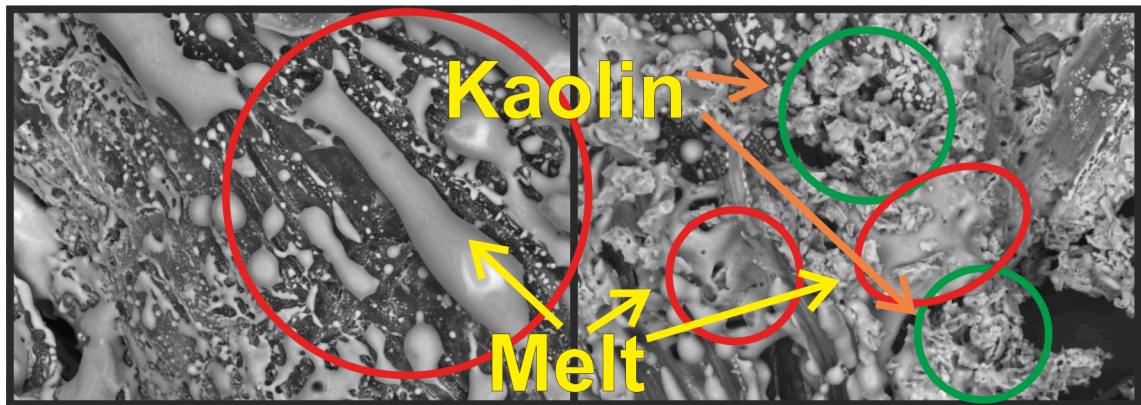

PICTURE 10. SEM pictures of pure wheat straw ash (left) and wheat straw with kaolin ash (right) from steam atmosphere at 850 $^{\circ}$C

The heterogeneous nature of the straw ash with MgO is clear on picture 11. Ash rich in silicon and sites with magnesium oxide powder are isolated from each other. This is further evidence that magnesium oxide works effectively to prevent sintering at least in this gas atmosphere (CO_2/Air-mixture). It is possible that in the tests runs in steam
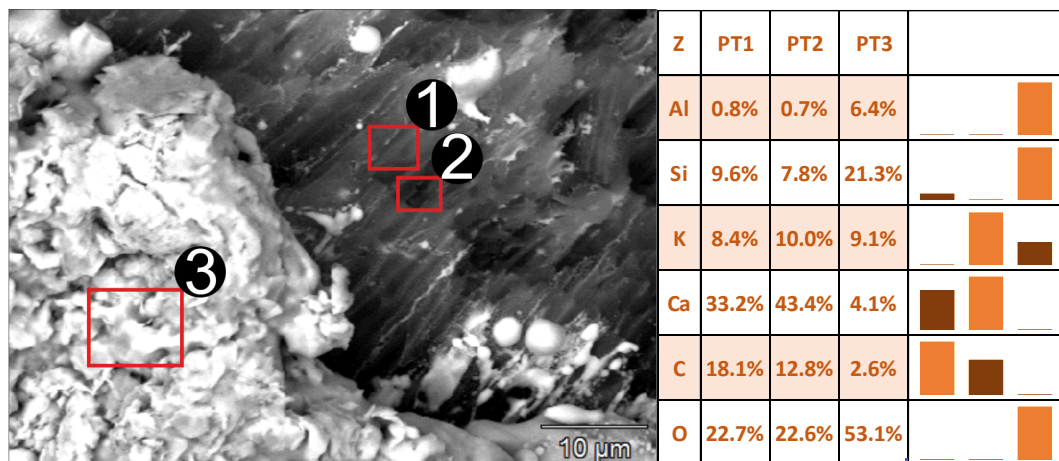
atmosphere water is mediating the formation of a thin layer of MgO on particles by rearrangement of its crystal structure.
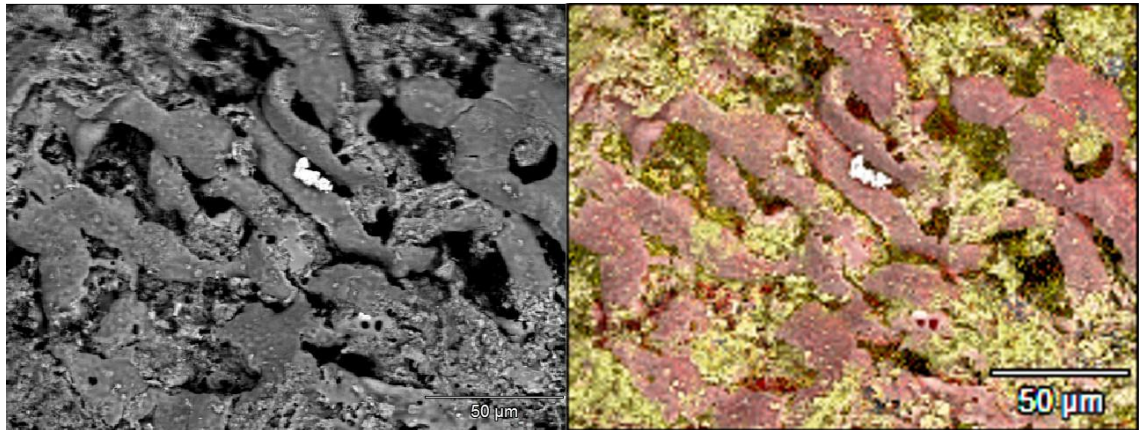
PICTURE 11. SEM picture (left) and EDS mapping of Si (red tint) and Mg (yellow tint) over original (right); Wheat straw doped with MgO from CO_2/Air-atmosphere at 950 ºC

During SEM inspection of wheat straw with kaolin ash sites of partially unreacted char were found (picture 12). EDS analysis clearly shows areas 1 and 2 have a high concentration of carbon and calcium, while area 3 has a relatively high concentration of aluminium and silicon. Potassium is expected to be found homogeneously on ash, while calcium is either removed or distributed during the reactions. Kaolin forms a layer on the char surface actually inhibiting some reaction sites. It is important to note that this layer is very soft and brittle, thus under any mechanical stress the results could be different.

Z	PT1	PT2	PT3
Al	0.8%	0.7%	6.4%
Si	9.6%	7.8%	21.3%
K	8.4%	10.0%	9.1%
Ca	33.2%	43.4%	4.1%
C	18.1%	12.8%	2.6%
O	22.7%	22.6%	53.1%

PICTURE 12. Kaolin doped wheat straw ash particle with partially unreacted char exposed (left); Summary of EDS analysis by wt.-% of relevant elements (right); Wheat straw doped with kaolin from CO_2/Air-atmosphere at 950 ºC

7 CONCLUSION

This work investigated the effect of MgO and kaolin on sintering behaviour when used as additives in wheat straw gasification. Using these additives was expected to reduce sintering due to their stability and inert chemical properties.

MgO reduces ash sintering in all cases, whilst increasing reactivity slightly in CO_2/Air-atmosphere gasification at higher temperatures. This seems to be a direct consequence of the reduced sintering allowing the reaction to proceed smoothly until the end. While MgO retains its crystal structure, and thus remains a fine granulate/powder, it appears to form slip sites which does not allow ash or molten particles to fuse together. Regardless of the test conditions MgO itself does seem to stay unfused and separate from the ash.

In steam gasification MgO behaves akin to kaolin, forming a thin layer in the surface of the particles. This layer formation is not homogeneous, with some particles being large and partially covered by MgO and others being quite small with granular MgO sites. Reactivity is reduced slightly, but not significantly, and from a practical point of view the reactivity is high and very similar to pure wheat straw. The formation of the MgO layer in the steam test run can be attributed to the interaction of steam with the MgO crystals, allowing the movement of lattices or the compactification of the granulates into a tighter formation. This would allow the homogeneous distribution of MgO forming a layer on top of the particles.

Kaolin inhibits ash sintering in all cases, whilst reducing reactivity slightly in CO_2/Air-atmosphere test runs and doubling conversion time in steam test runs. In all cases kaolin seems to form a thin layer over char and ash inhibiting conversion. This layer formation in kaolin could be triggered by the thermochemical decomposition of kaolin into metakaolin at lower temperatures (over 625 $^{\circ}$C), which has longer range order in its crystal structure. The early formation of the layer in the test run coupled with the steam mediating inter-particle interaction could explain the significantly lower reactivity in steam atmosphere test runs. In CO_2/Air-atmosphere test runs kaolin forms layers over ash and char, but reactivity is not affected significantly. The high reactivity and lack of steam could be enough to allow the char to react before the formation of an inhibiting layer of kaolin.

On the conditions studied in this work both kaolin and MgO work effectively in reducing sintering. This is more accentuated in higher temperatures, where the sintering of ash would otherwise be very high. Results obtained in this work conformed to the expected behaviour, and are encouraging for further testing.

Future Work

Considering the test conditions used in this work, the next stepping point would be to either expand this analysis to a somewhat larger scale with larger sample sizes, of 1 to 10 g, or expanding the test points to include a wider range of conditions. Larger scale tests which allow movement of the sample might represent better the conditions in a real gasifier.

Considering the reactivity behaviour of the samples under different gas atmospheres, expanding the test-matrix herein to include the additives in all atmospheres and the full temperature gradient could explain better the interactions of these additives with the samples. For this test points to be useful the use of SEM and EDS has a very central role, and even a quick mapping of the surface of ash can present data otherwise impossible to get.

Investigation of both MgO and kaolin additives on bench-scale fixed-bed tests is necessary to confirm the sintering behaviour of wheat straw in cases where accumulation of ash is actually significant, the results here-in present a small subset of the possible physical interactions ash might undergo in a reactor due to the mechanically static and very small sample size.

In this work the study of only wheat straw as the feedstock is justified because it presents a highly available agricultural residue. For the future, including other problematic feedstock is necessary to observe consistent behaviour regardless of ash composition. On the longer term this seem to be the most appropriate course of action in impacting the fuel flexibility of small scale gasification.

REFERENCES

Basu, P. (2010a). Introduction. Biomass Gasification and Pyrolysis - Practical Design and Theory. Elsevier. 1–25. http://doi.org/10.1016/B978-0-12-374988-8.00001-5

Basu, P. (2010b). Biomass Characteristics. Biomass Gasification and Pyrolysis - Practical Design and Theory. Elsevier. 27–63. http://doi.org/10.1016/B978-0-12-374988-8.00002-7

Bocci, E., Sisinni, M., Moneti, M., Vecchione, L., Di Carlo, A. & Villarini, M. (2014). State of art of small scale biomass gasification power systems: A review of the different typologies. Energy Procedia, 45, 247–256. http://doi.org/10.1016/j.egypro.2014.01.027

European Commission. (2015). EU energy in figures, STATISTICAL POCKETBOOK 2015. Luxembourg: Publications Office of the European Union. p. 29. http://doi.org/10.2833/77358

European Commission. (2010). Report from the Commission to the Council and the European Parliament on sustainability requirements for the use of solid and gaseous biomass sources in electricity, heating and cooling SEC (2010) 65 final SEC (2010) 66 final. http://eur-lex.europa.eu/legal-content/EN/NOT/?uri=CELEX:52010DC0011

European Commission. (2014). State of play on the sustainability of solid and gaseous biomass used for electricity, heating and cooling in the EU.

European Environment Agency. (2013). EU bioenergy potential from a resource-efficiency perspective. http://doi.org/10.2800/92247

Kirkels, A. F. & Verbong, G. P. J. (2011). Biomass gasification: Still promising? A 30-year global overview. Renewable and Sustainable Energy Reviews, 15(1), 471–481. http://doi.org/10.1016/j.rser.2010.09.046

Moilanen, A. (2010). Kaasutuksen perusteet. In AEL Insko-seminaari 15-16.9.2010. Helsinki.

Moilanen, A. (2006). Thermogravimetric characterisations of biomass and waste for gasification processes. VTT Publications 607, 103 p. + app. 97 p. www.vtt.fi/inf/pdf/publications/2006/P607.pdf

Moilanen, A. & Nasrullah, M. (2011). Gasification reactivity and ash sintering behaviour of biomass feedstocks. VTT Publications 769. 39 p. + app. 96 p. www.vtt.fi/inf/pdf/publications/2011/P769.pdf

Nakamura, K., Miyazawa, T., Sakurai, T., Miyao, T., Naito, S., Begum, N., Kunimori, K. & Tomishige, K. (2009). Promoting effect of MgO addition to Pt/Ni/CeO2/Al2O3 in the steam gasification of biomass. Applied Catalysis B: Environmental, 86(1-2), 36–44. http://doi.org/10.1016/j.apcatb.2008.07.016

Perander, M., DeMartini, N., Brink, A., Kramb, J., Karlström, O., Hemming, J., Moilanen, A., Konttinen, J. & Hupa, M. (2015). Catalytic effect of Ca and K on CO2 gasification of spruce wood char. Fuel, 150, 464–472. http://doi.org/10.1016/j.fuel.2015.02.062

Pereira, E. G., Da Silva, J. N., De Oliveira, J. L. & Machado, C. S. (2012). Sustainable energy: A review of gasification technologies. Renewable and Sustainable Energy Reviews, 16(7), 4753–4762. http://doi.org/10.1016/j.rser.2012.04.023

Skrifvars, B.-J., Backman, R. & Hupa, M. (1998). Characterization of the sintering tendency of ten biomass ashes in FBC conditions by a laboratory test and by phase equilibrium calculations. Fuel Processing Technology, 56(1-2), 55–67. http://doi.org/10.1016/S0378-3820(97)00084-2

Sources of biomass. Biomass Energy Centre UK. Read April 12, 2016, from http://www.biomassenergycentre.org.uk/portal/page?_pageid=75,15174&_dad=portal&_schema=PORTAL

Wilén, C., Moilanen, A. & Kurkela, E. (1996). Biomass feedstock analyses. VTT Publications 282. 25 p. + app. 8 p. www.vtt.fi/inf/pdf/publications/1996/P282.pdf

Xu, G., Murakami, T., Suda, T., Kusama, S. & Fujimori, T. (2005). Distinctive effects of CaO additive on atmospheric gasification of biomass at different temperatures. Industrial and Engineering Chemistry Research, 44(15), 5864–5868. http://doi.org/10.1021/ie050432o

APPENDICES

Appendix 1. Summary of the feedstock analysis

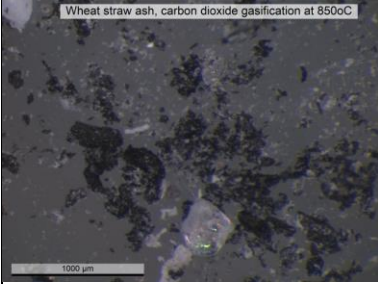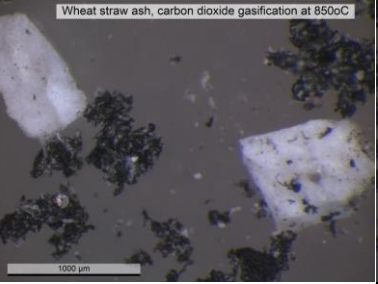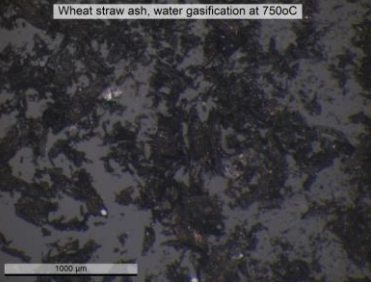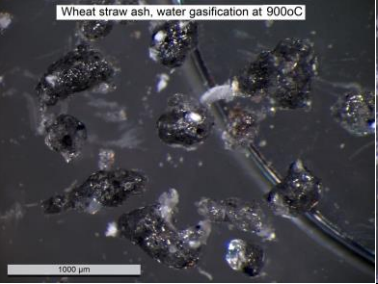|	Wheat straw	Wheat straw + 4.5% kaolin	Wheat straw + 4.5% MgO
	[wt.-%]		
Moisture	8.3	8.6	8.6
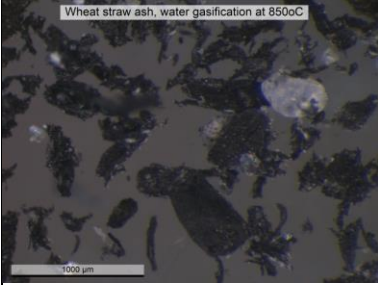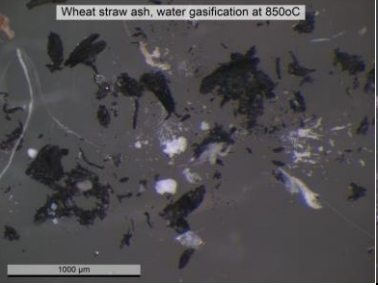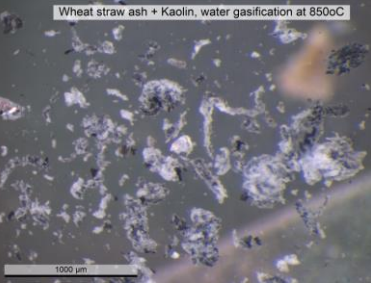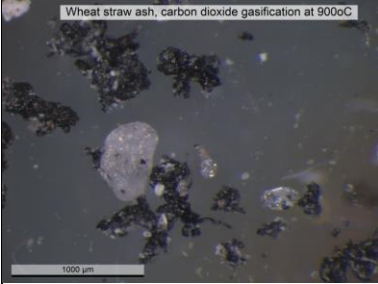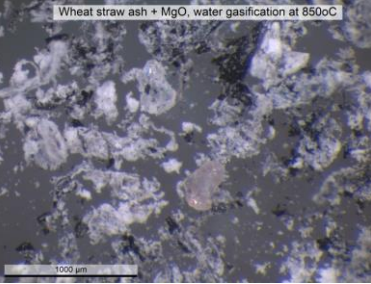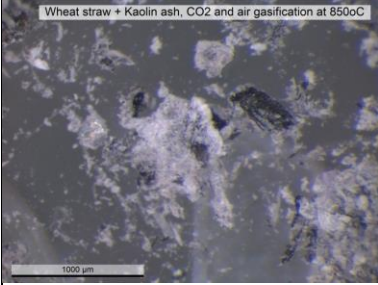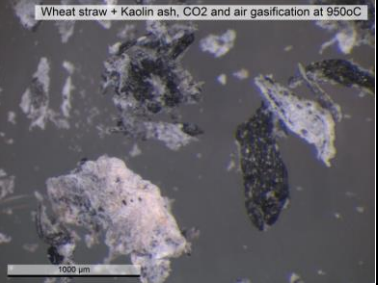
	Wheat straw	Wheat straw + 4.5% kaolin	Wheat straw + 4.5% MgO
	In dry matter [wt.-%]		
C	46.1	44.7	44.8
H	5.6	5.5	5.4
N	0.8	0.8	0.8
Ash (550°C)	6.5	9.2	9.1

	Wheat straw	Wheat straw + 4.5% kaolin	Wheat straw + 4.5% MgO [*]
	In dry matter [mg/kg] (analyzed by ICP method)		
Cl	5600	2900	4000
Na	4500	3100	3200
K	109500	84200	78200
Ca	70000	50400	50000
Mg	10000	8800	181400
P	19700	14200	14100
S	9500	5200	6800
Al	7500	68200	5400
Si	277700	272200	198400
Fe	8700	7500	6200
Ti	380	1400	270
Cr	67	47	48
Cu	57	43	41
Mn	520	350	370
Ni	13	10	9
Zn	220	170	160
Ba	830	680	590
Sb	0.77	0.70	0.55
As	1.8	2.5	1.3
Cd	3.0	1.4	2.1
F	390	550	280
Br	<0,025	<0,025	<0,025
Co	2.8	1.9	2.0
Pb	20	37	14
Mo	14	8.7	10.0
Se	3	6.3	2.1
Tl	<0,5	<0,5	<0,5
Sn	0.93	4.1	0.66
V	12	20	9
Hg	0.13	0.08	0.09
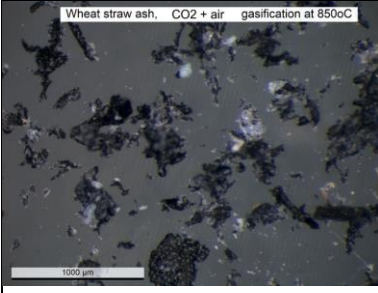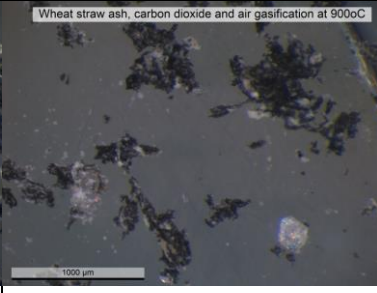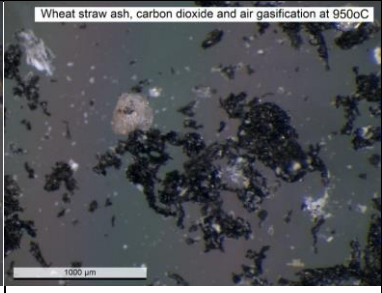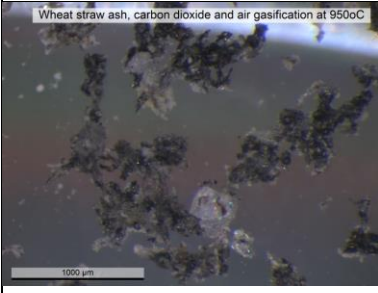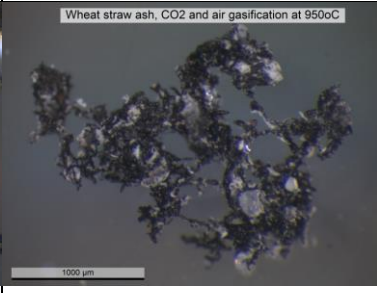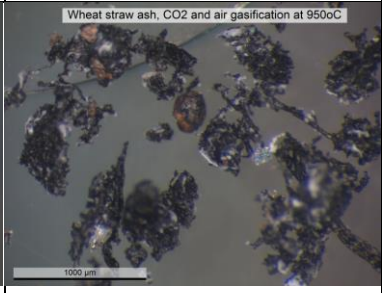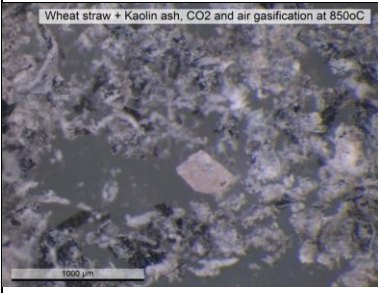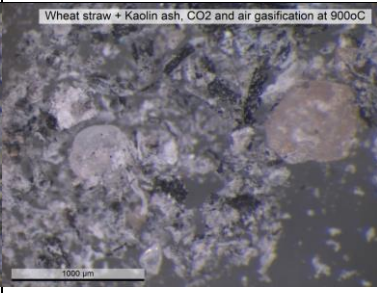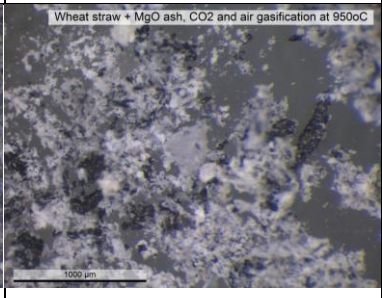
[*] Ash composition has been calculated based on the straw ash composition and the amount of added MgO

Appendix 2. Microscopy photographs

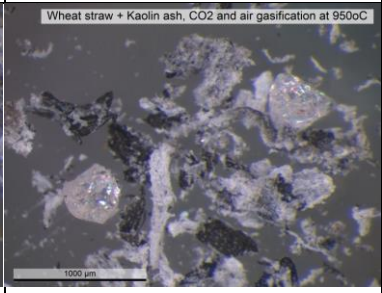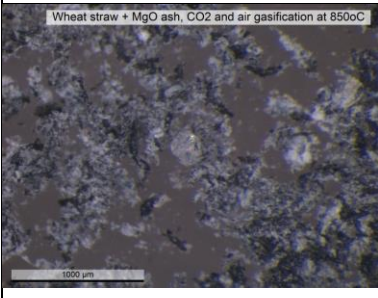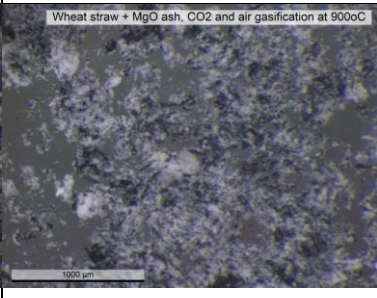| WS – CO$_2$ atmosphere at 850 $^{\circ}$C – *(*) (A)	WS – CO$_2$ atmosphere at 850 $^{\circ}$C – *(*) (B) Impurities	WS – Steam atmosphere at 750 $^{\circ}$C – O
Wheat straw ash, carbon dioxide gasification at 850oC	Wheat straw ash, carbon dioxide gasification at 850oC	Wheat straw ash, water gasification at 750oC
WS – Steam atmosphere at 850 $^{\circ}$C – *(*) (A)	WS – Steam atmosphere at 850 $^{\circ}$C – *(*) (B)	WS + kaolin – Steam atmosphere at 850 $^{\circ}$C – (*) (A)
Wheat straw ash, water gasification at 850oC	Wheat straw ash, water gasification at 850oC	Wheat straw ash + Kaolin, water gasification at 850oC
WS – CO$_2$ atmosphere at 900 $^{\circ}$C – **	WS – Steam atmosphere at 900 $^{\circ}$C – ***	WS + MgO – Steam atmosphere at 850 $^{\circ}$C – (*)
Wheat straw ash, carbon dioxide gasification at 900oC	Wheat straw ash, water gasification at 900oC	Wheat straw ash + MgO, water gasification at 850oC
WS + kaolin – CO$_2$/Air- atmosphere at 850 $^{\circ}$C – (*) (B) Cover	WS + kaolin – CO$_2$/Air- atmosphere at 950 $^{\circ}$C – (*) (B) Cover	
Wheat straw + Kaolin ash, CO2 and air gasification at 850oC	Wheat straw + Kaolin ash, CO2 and air gasification at 950oC	**WS = wheat straw**

(continues)

WS – CO$_2$/Air-atmosphere at 850 ºC – *	WS – CO$_2$/Air-atmosphere at 900 ºC – *(*)	WS – CO$_2$/Air-atmosphere at 950 ºC – ** (A)
WS – CO$_2$/Air-atmosphere at 950 ºC – **(*) (B)	WS – CO$_2$/Air-atmosphere at 950 ºC – ** (C)	WS – CO$_2$/Air-atmosphere at 950 ºC – ** (D)
WS + kaolin – CO$_2$/Air-atmosphere at 850 ºC – (*)	WS + kaolin – CO$_2$/Air-atmosphere at 900 ºC – (*)	WS + kaolin – CO$_2$/Air-atmosphere at 950 ºC – (*)
WS + MgO – CO$_2$/Air-atmosphere at 850 ºC – O, mp	WS + MgO – CO$_2$/Air-atmosphere at 900 ºC – O, mp	WS + MgO – CO$_2$/Air-atmosphere at 950 ºC – O, mp

Appendix 3. Summary of results with run numbers for later reference

RUN #	Fuel	Gas	Temp [°C]	Xt-99% [min]	R@90% [%/min]	SD	Rating	Ash [wt.-%]	SEM	EDS	Status
692	PWS	Steam	750	>110	2.6	O	--	8.46	N	N	
644	PWS	Steam	850	14	36	N	N	5.58	X	X	EXTRA
674	PWS	Steam	850	13.2	34	*(*)	O	6.17	N	N	
671	PWS	Steam	900	4.8	88	*(*)	O	5.96	X	N	
665b	PWS	CO2	850	N	N	*(*)	O	5.82	N	N	EXTRA
665	PWS	CO2	850	10.8	22	*(*)	O	5.51	N	N	
670	PWS	CO2	900	5.8	50	**	-	5.63	N	N	
677	PWS	CO2/Air	850	1.55	160	*	+	5.94	N	N	
669	PWS	CO2/Air	900	1.28	210	*(*)	O	6.05	N	N	
681	PWS	CO2/Air	950	N	N	**	-	6.22	N	N	EXTRA
695	PWS	CO2/Air	950	N	N	**(*)	--	6.28	X	N	EXTRA
696	PWS	CO2/Air	950	1.13	303	**	-	5.63	N	N	
675	PWS + MgO	CO2/Air	850	1.55	164	O, mp	++	8.19	N	N	
676	PWS + MgO	CO2/Air	900	1.25	205	O, mp	++	8.13	N	N	
683	PWS + MgO	CO2/Air	950	1.02	329	O, mp	++	8.01	X	X	
678	PWS + Kaolin	CO2/Air	850	1.68	145	(*)	++	7.93	N	N	
679	PWS + Kaolin	CO2/Air	900	1.42	186	(*)	++	7.97	N	N	
684	PWS + Kaolin	CO2/Air	950	1.14	246	(*)	++	7.40	X	X	
693	PWS + MgO	Steam	850	13.2	30	(*)	++	8.04	N	N	
646	PWS + Kaolin	Steam	850	4.8	26	(*)	++	7.14	X	X	

Xt-99% = time until 99% fuel conversion is reached [min]   R@90% = reactivity at 90% fuel conversion stage [% / min]

SD = sintering degree   mp = molten particles   PWS = pure wheat straw   SEM = scanning electron microscope analysis

Rating = sintering degree compared to steam gasification at 850°C (--, -, O, +, ++)   EDS = energy dispersive x-ray spectroscopy

EXTRA = extra run, incomplete analysis   X = analyzed   N = not analyzed